ALMA MATER STUDIORUM
UNIVERSITÀ DI BOLOGNA

Instrumental Monitoring for Natural Hazards: Landslides and Tsunamis

Cesare Angeli[1], **Martina Zanetti**[1], Alberto Armigliato[1], Filippo Zaniboni[1], Enrico Paolucci[1]

[1]*Department of Physics and Astronomy "A. Righi", Alma Mater Studiorum - University of Bologna, Bologna, Italy*

OUTLOOK

- What is a **mud volcano**? Why do we study them?
- The case of **Salse del Dragone**
- How we investigated it: **seismic surveys & modelling**
- What we learned and why it matters

Where do we find mud volcanoes?

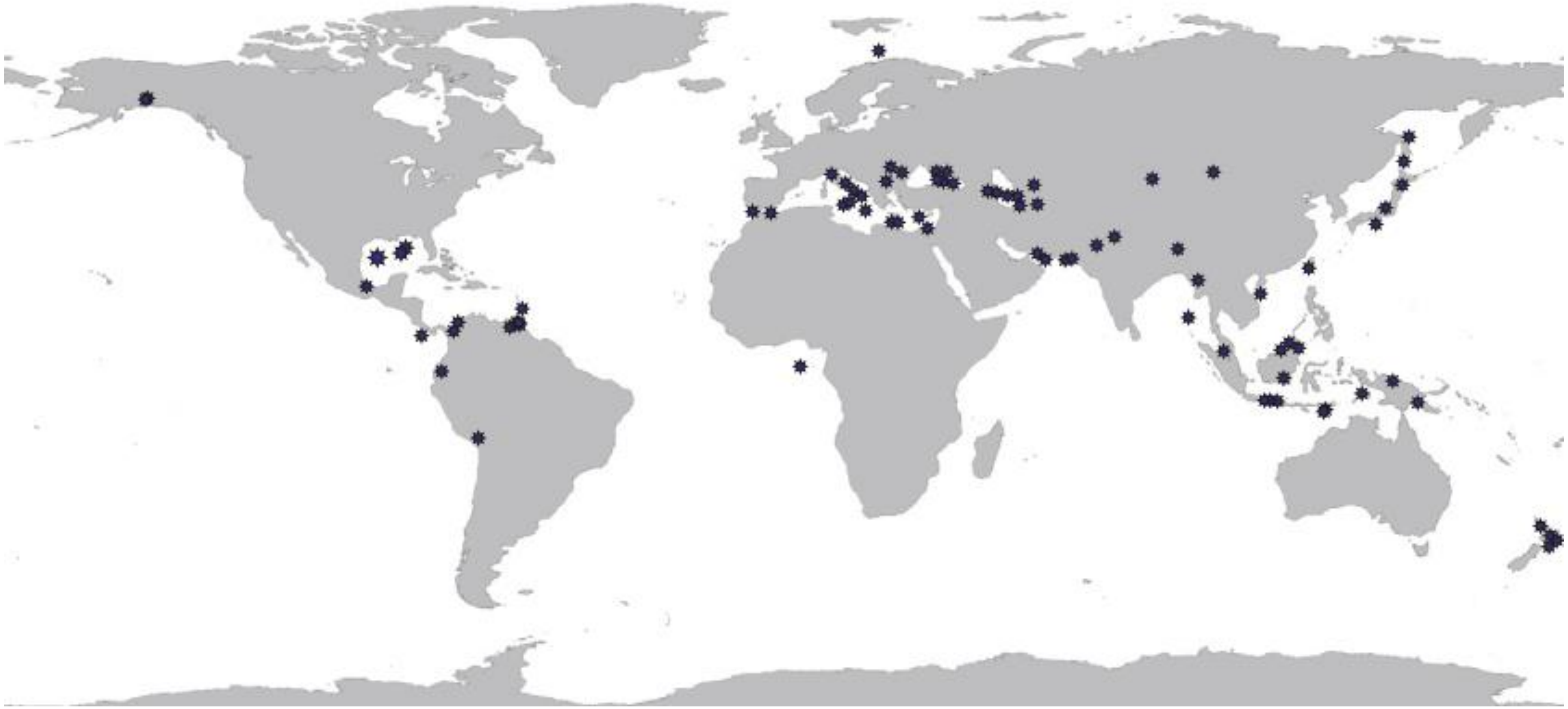

Global distribution of mud volcanoes (Mazzini and Etiope, 2017)

- Broadly distributed throughout the globe in active and passive margins, deep sedimentary basins related to active plate boundaries, as well as delta regions: primarily located **in petroliferous basins** and associated with **petroleum systems**
- Estimated 900 onshore and 800 offshore MVs worldwide (Dimitrov, 2002)
- ~200 structures in both Romania and Azerbaijan

Where do we find mud volcanoes?

Located in three main areas: the **northern Apennines** (Emilia-Romagna region), the **central Apennines** (Marche and Abruzzo), and **Sicily**

Salse di Nirano

Maccalube di Aragona
(2014 event: 2 fatalities)

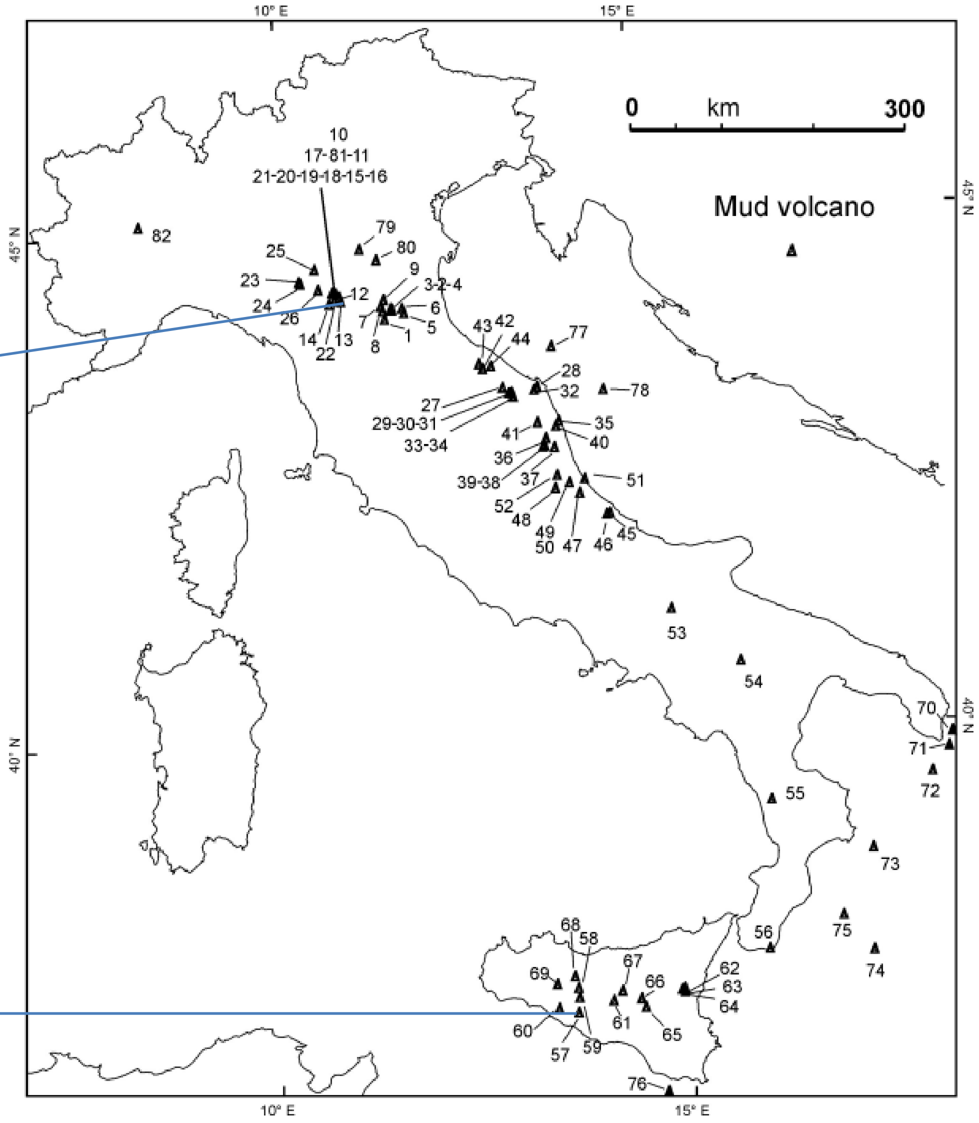

Italian distribution of mud volcanoes (Martinelli et al., 2012)

Mud volcanoes

Mazzini and Etiope, 2017

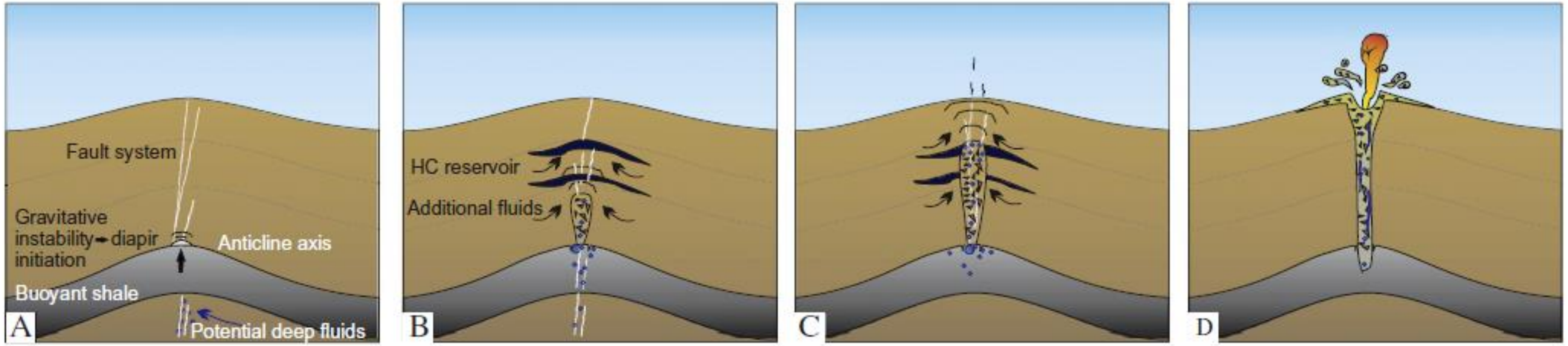

The study of mud volcanoes and their emission activities have significant implications in terms of:

- **energy resource exploration**
- **atmospheric budget of greenhouse gases**
- **geohazard assessment**

The Salse del Dragone case study

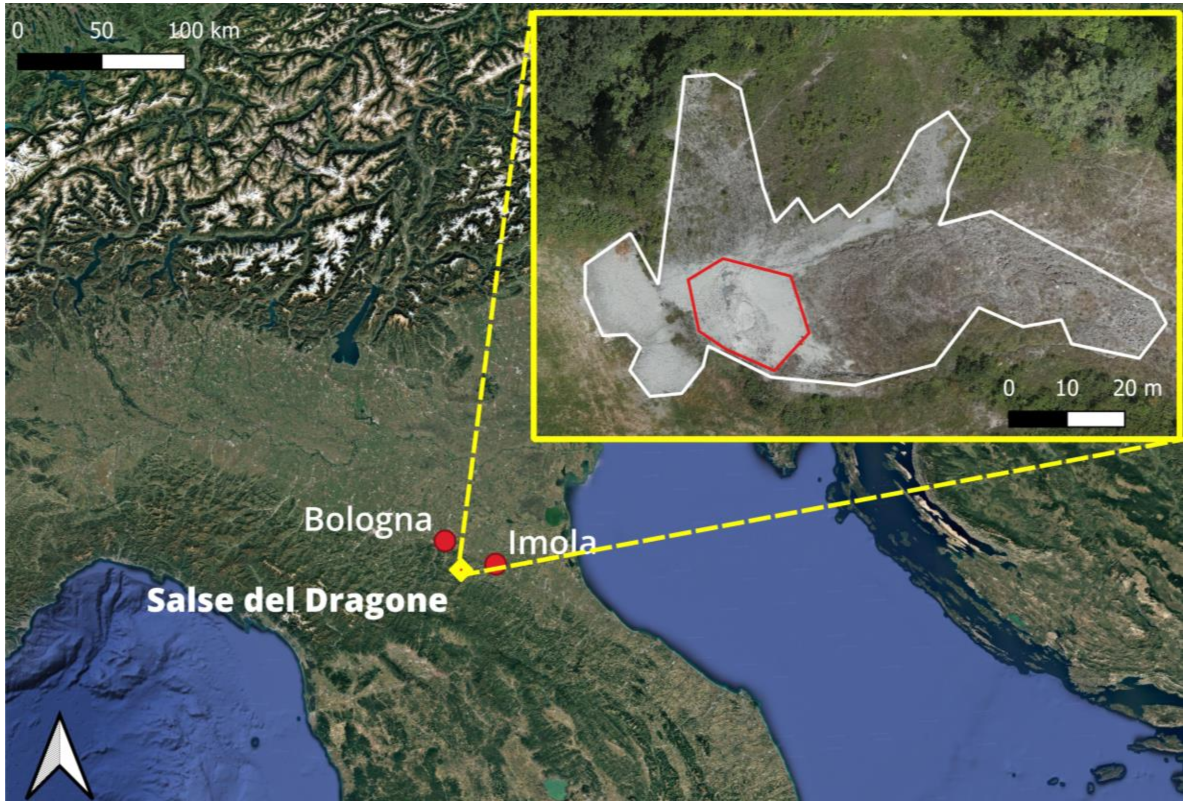

Mud plateau of about 200 m² surrounded by 1500 m² of mud deposit.

The name "Dragone," meaning "The Dragon," comes from the fact that their activity was reportedly much more vigorous in the past (the 1800s), with eruptions reaching tens of meters, as recorded by the mineralogist Luigi Bombicci.

ALMA MATER STUDIORUM
UNIVERSITÀ DI BOLOGNA

The Salse del Dragone case study

Professor Marco Antonellini retrieving
mud samples from the crater area.

Zoom of the drilled
hole for sample acquisitions.

The Salse del Dragone case study

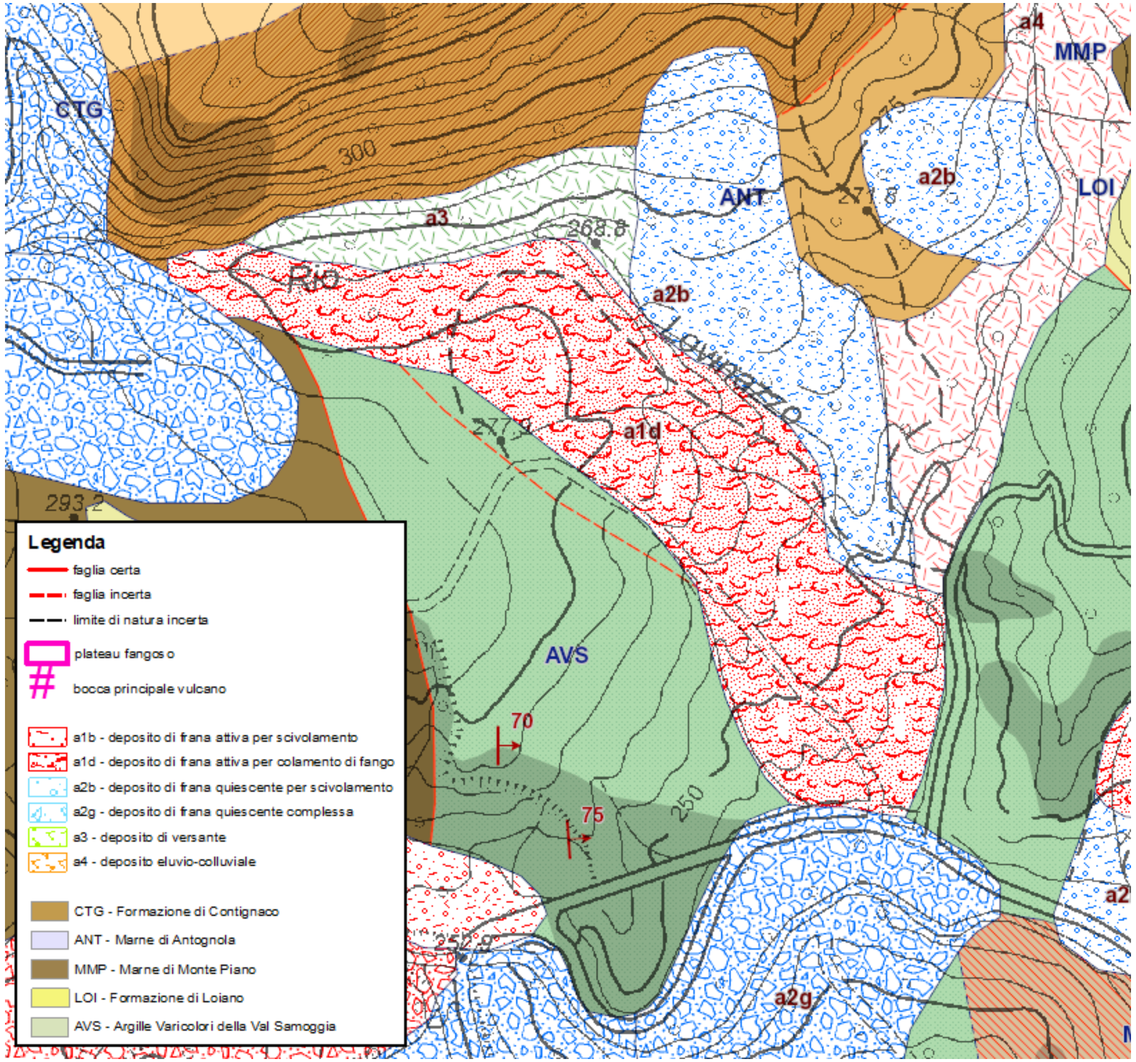

Regional Geological Map of Emilia Romagna region
(https://servizimoka.regione.emilia-romagna.it/)

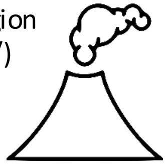

IS THIS A REAL LANDSLIDE?

ALMA MATER STUDIORUM
UNIVERSITÀ DI BOLOGNA

Subsurface characterization through seismic surveys

BODY WAVES

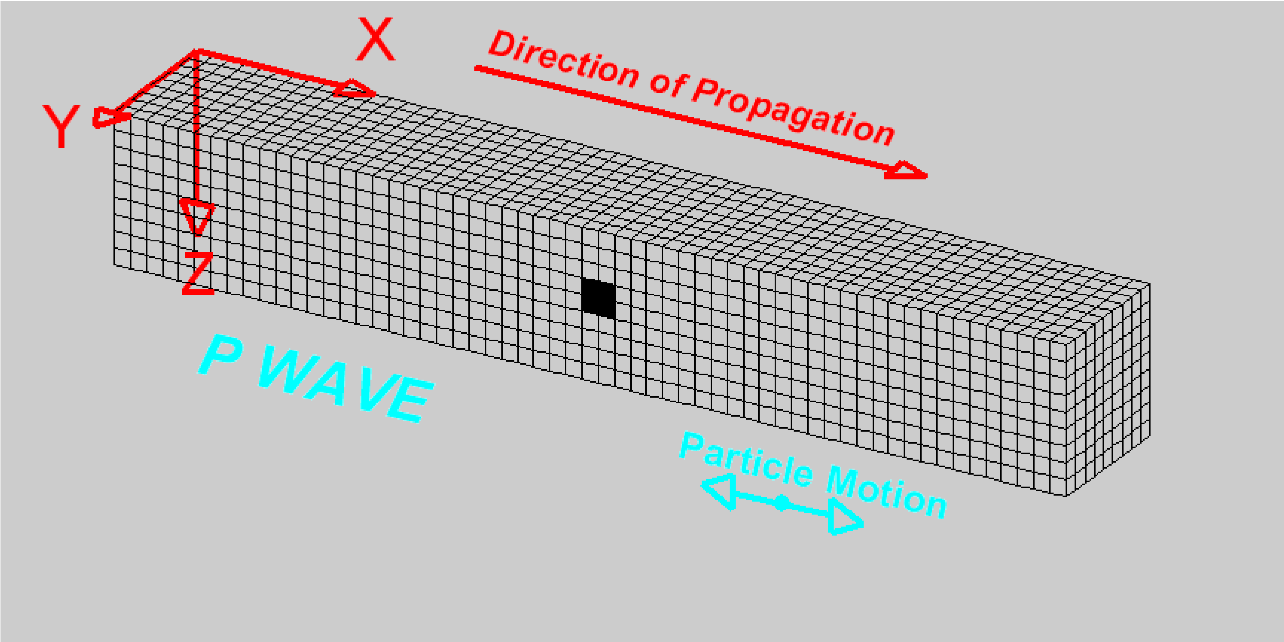

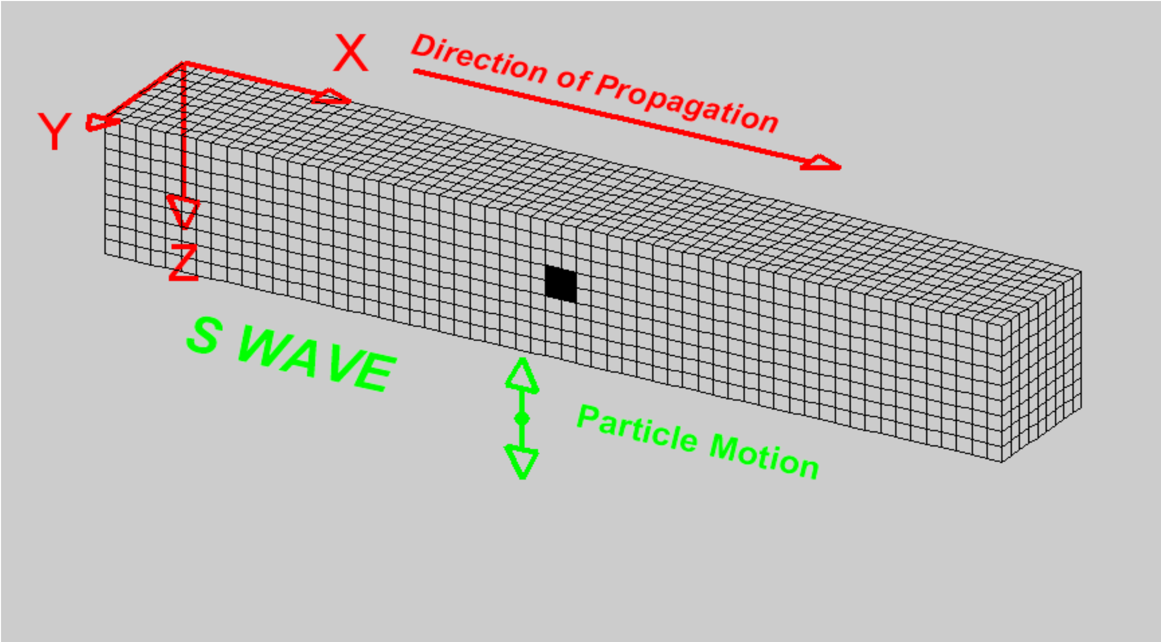

$$V_P = \sqrt{\frac{K+\frac{4}{3}G}{\rho}}$$

K = Bulk modulus
G = Shear modulus
ρ = Density
ν = Poisson's ratio (typically 0.2–0.5)

$$V_S = \sqrt{\frac{G}{\rho}}$$

Subsurface layering is investigated through a **Vs profile as a function of depth**

Subsurface characterization through seismic surveys

SURFACE WAVES

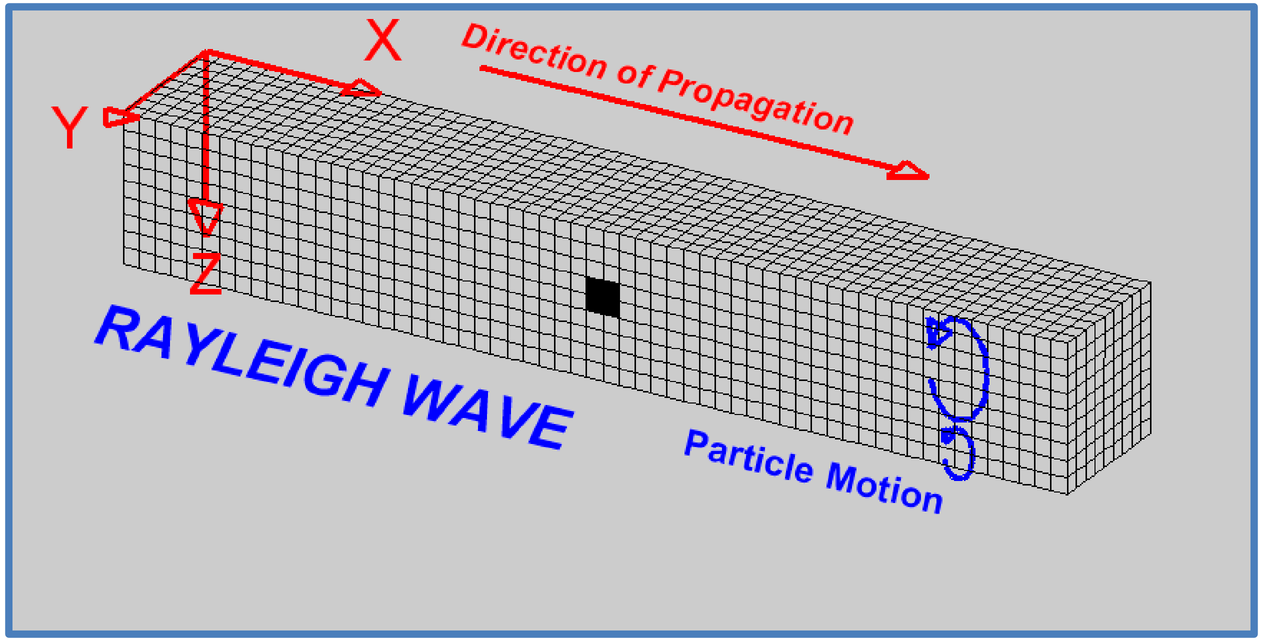

Retrograde elliptical motion

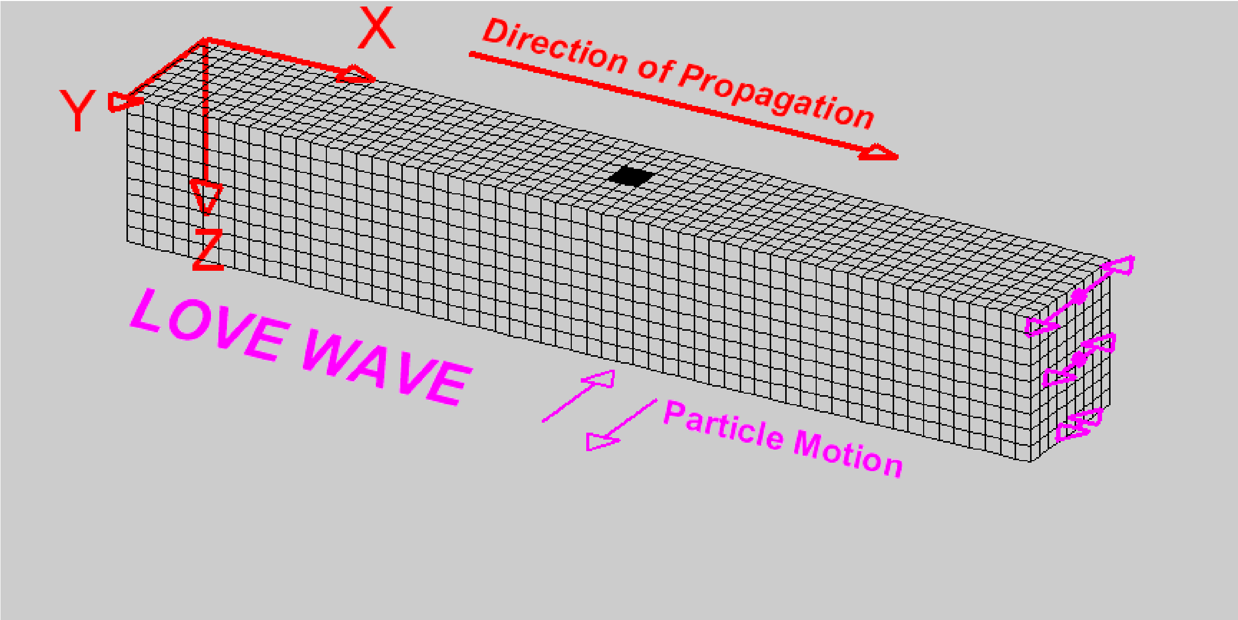

Horizontal motion transverse to the direction of propagation

- They can be recorded using vertical geophones (a very common type of instrumentation).
- The velocity of Rayleigh waves (VR) essentially depends on the shear wave velocity.

$$V_R \approx \left(\frac{0.874 + 1.117\nu}{1 + \nu}\right) V_S$$

ALMA MATER STUDIORUM UNIVERSITÀ DI BOLOGNA

Instrumental set up (arrays)

Seismic array measurements were carried out using SoilSpy Rosina™ digital acquisition system produced by MoHo s.r.l. (https://moho.world/en/soilspy/) equipped with 16 - 4.5 Hz vertical geophones (sensors that detect and record ground vibrations).

Used for both active and passive seismic measurements.

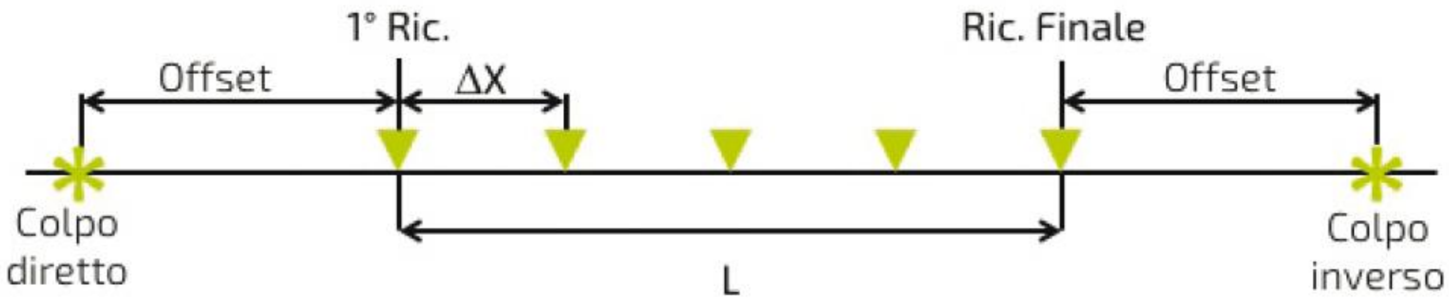

Instrumental set up (single station)

Three-directional 24-bit digital tromograph **Tromino™** produced by MoHo s.r.l. (https://moho.world/en/tromino/)

It measures ground motion in three directions (vertical, North-South, East-West) and is commonly used to estimate the resonance frequency of soil through HVSR (Horizontal-to-Vertical Spectral Ratio) analysis.

Used for passive seismic measurements, particularly **ambient noise recordings** (amplitudes on the order of 10^{-4} to 10^{-2} mm)

Subsurface characterization through seismic surveys

Roman testudo

Vertically heterogeneous medium

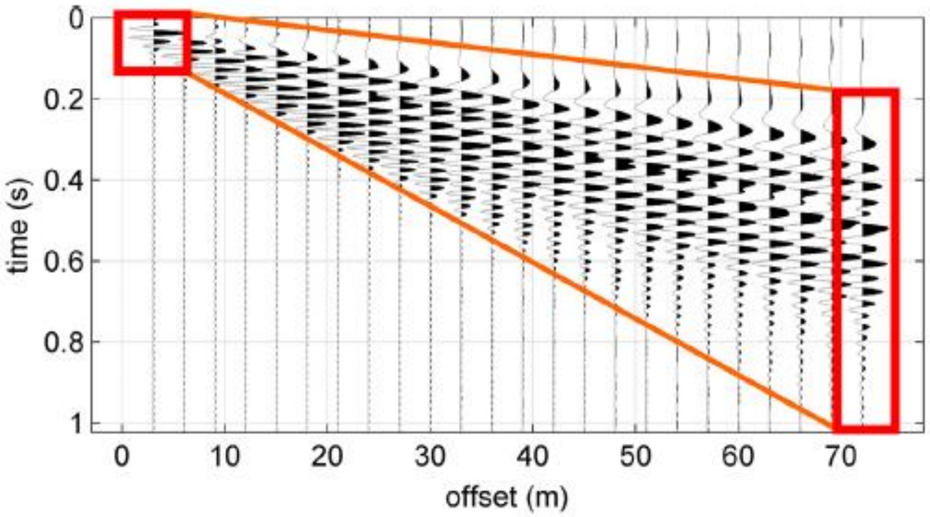

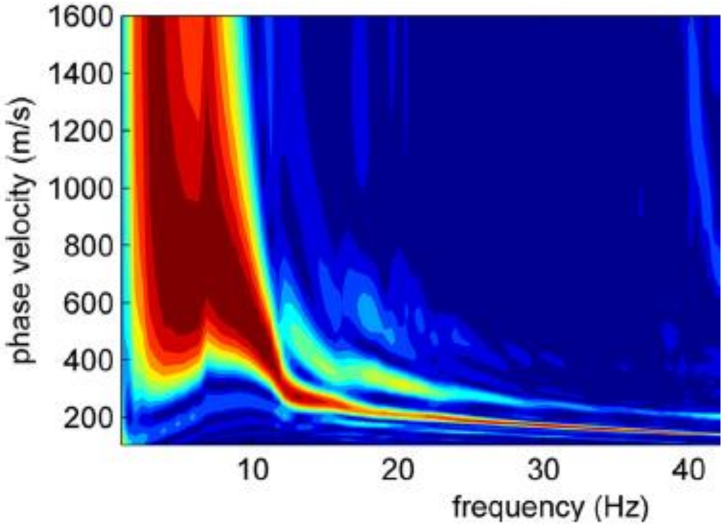

Vertically homogeneous medium

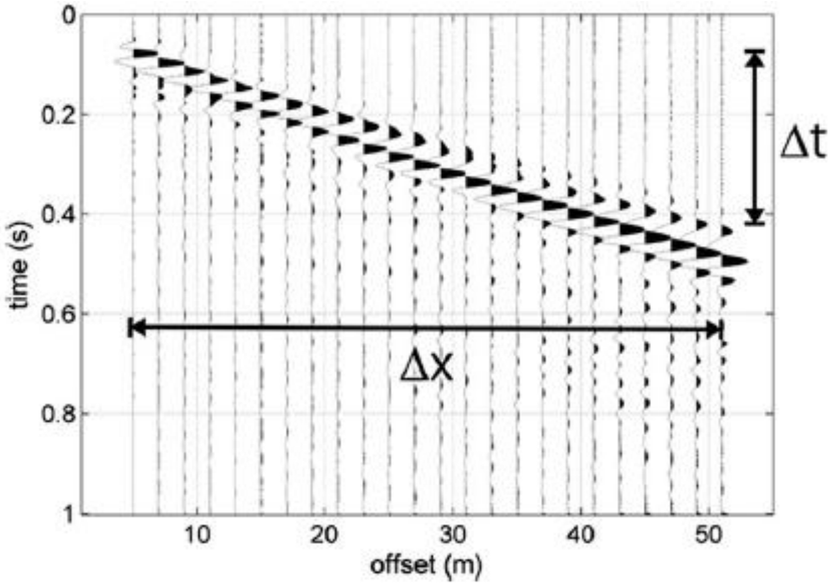

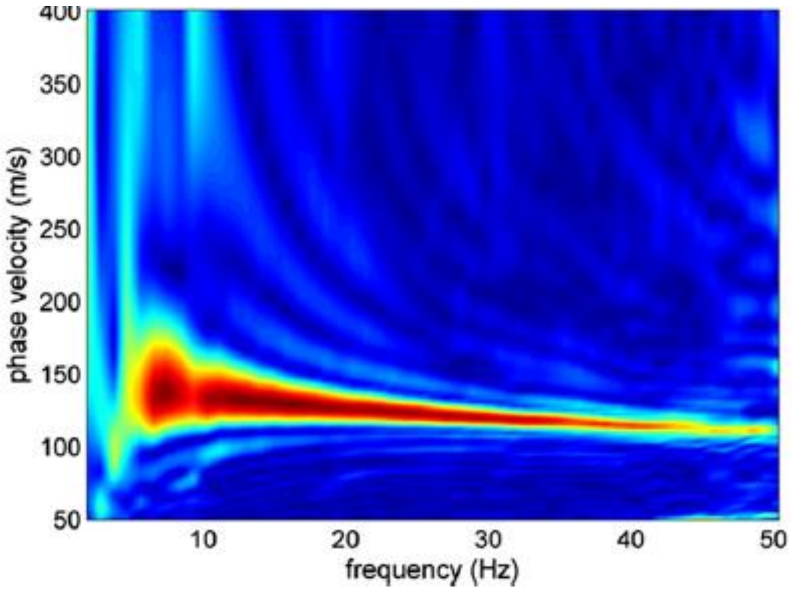

(Dal Moro, 2015)

Subsurface characterization through seismic surveys

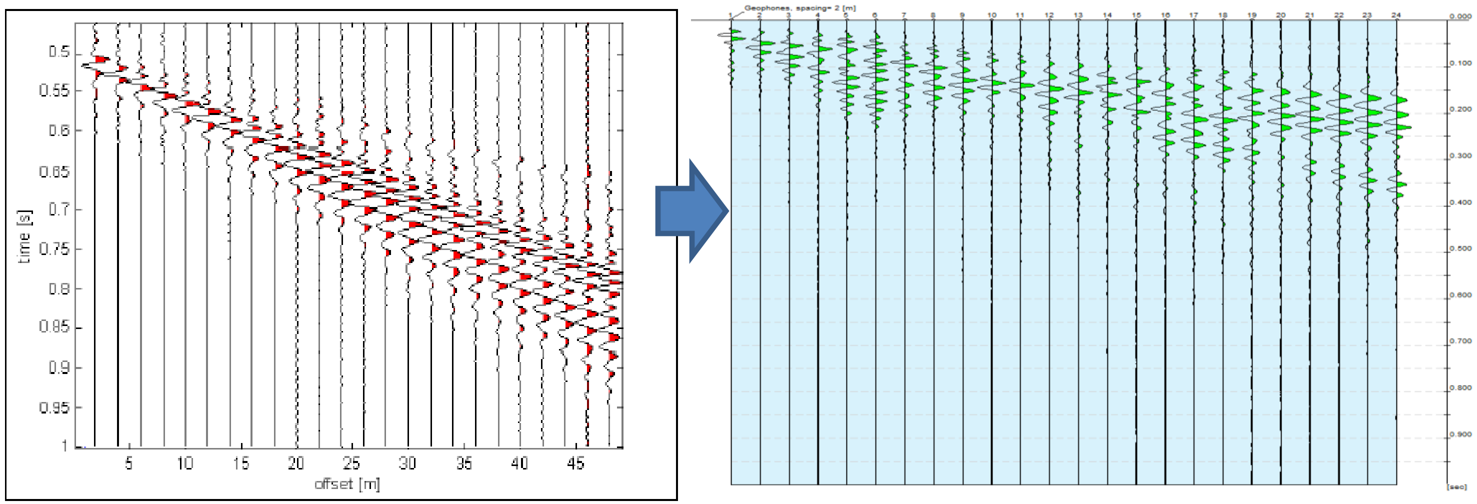

The signal recorded at each geophone is filtered to isolate a narrow range of vibration frequencies (band-pass filter).

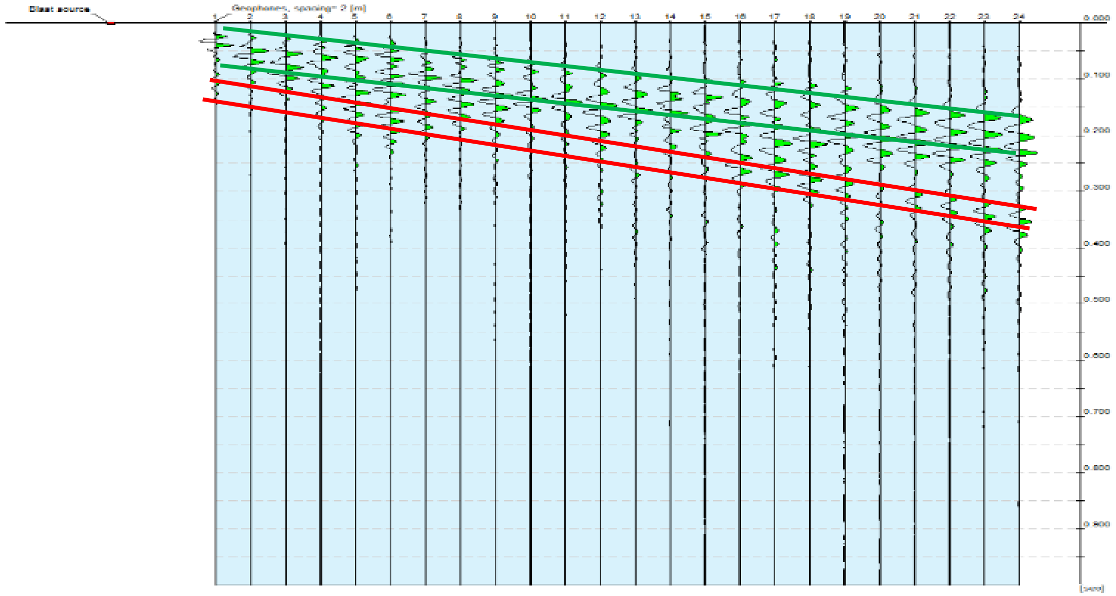

The propagation of a single phase appears as a straight line on the offset–time graph. Amplitude values are then stacked along different sloped bands (**slant stack**), each corresponding to a different possible propagation velocity.

The higher the stacking value (S), the greater the coherence associated with that velocity.

Other analysis methods exist besides slant-stack (such as f–k methods, phase shift, etc.), but the results are generally similar.

Subsurface characterization through seismic surveys

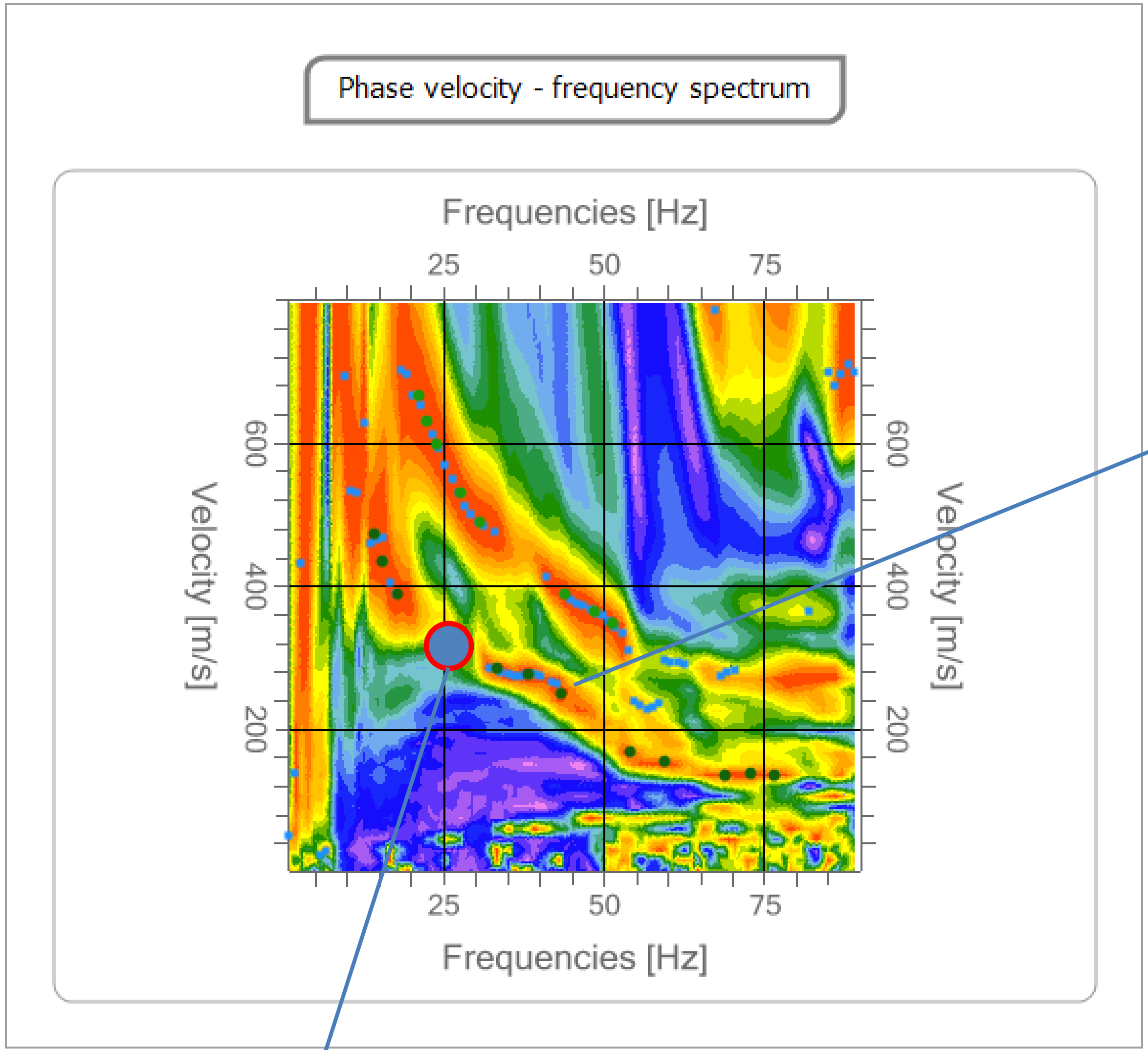

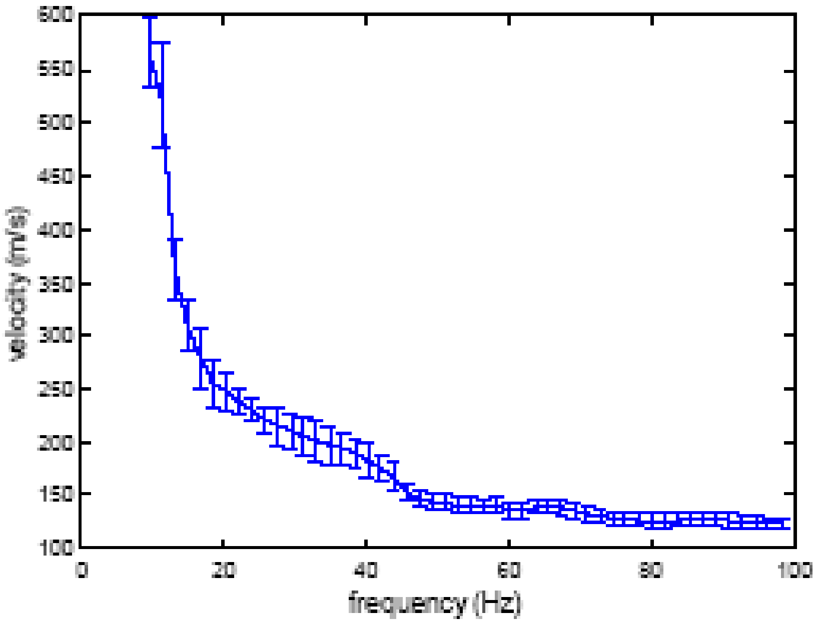

Multiple inversion algorithms can be applied to retrieve Vs profiles from surface wave data. While methodologies differ (e.g., linearized, stochastic, or global search), they all aim to minimize the misfit between observed and synthetic data

Stacking value (S) for a frequency of 25 Hz and a trial velocity of 350 m/s

Seismic Surveys: Results

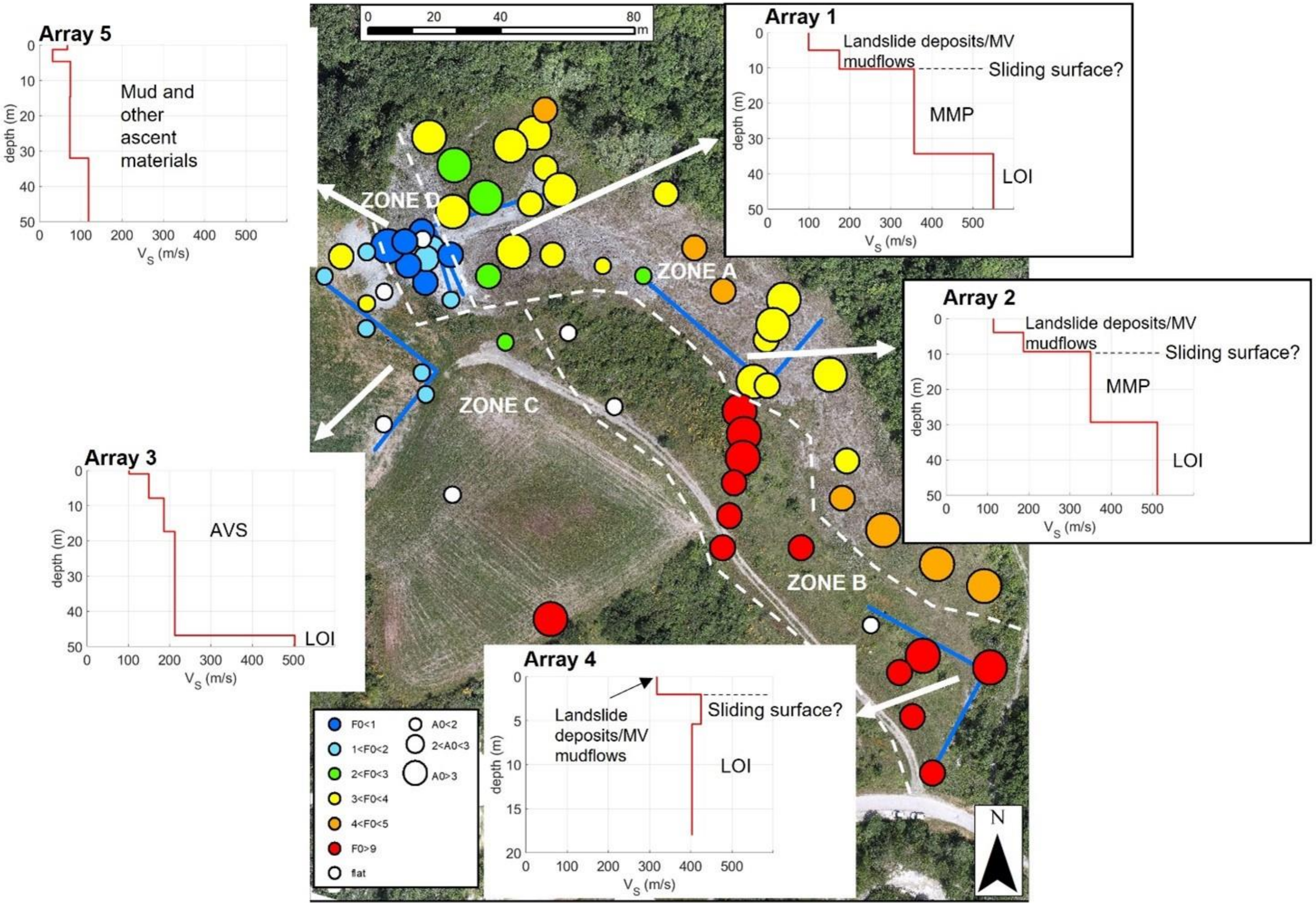

68 single stations (passive)
Time length 20 min
Three-directional sensors

5 seismic arrays (passive)
Time length 30-40 min
16 vertical geophones
C or L-shape layout

5 MASW (active)
10-16 vertical geophones
Linear layout

ALMA MATER STUDIORUM
UNIVERSITÀ DI BOLOGNA

Seismic Surveys: Results

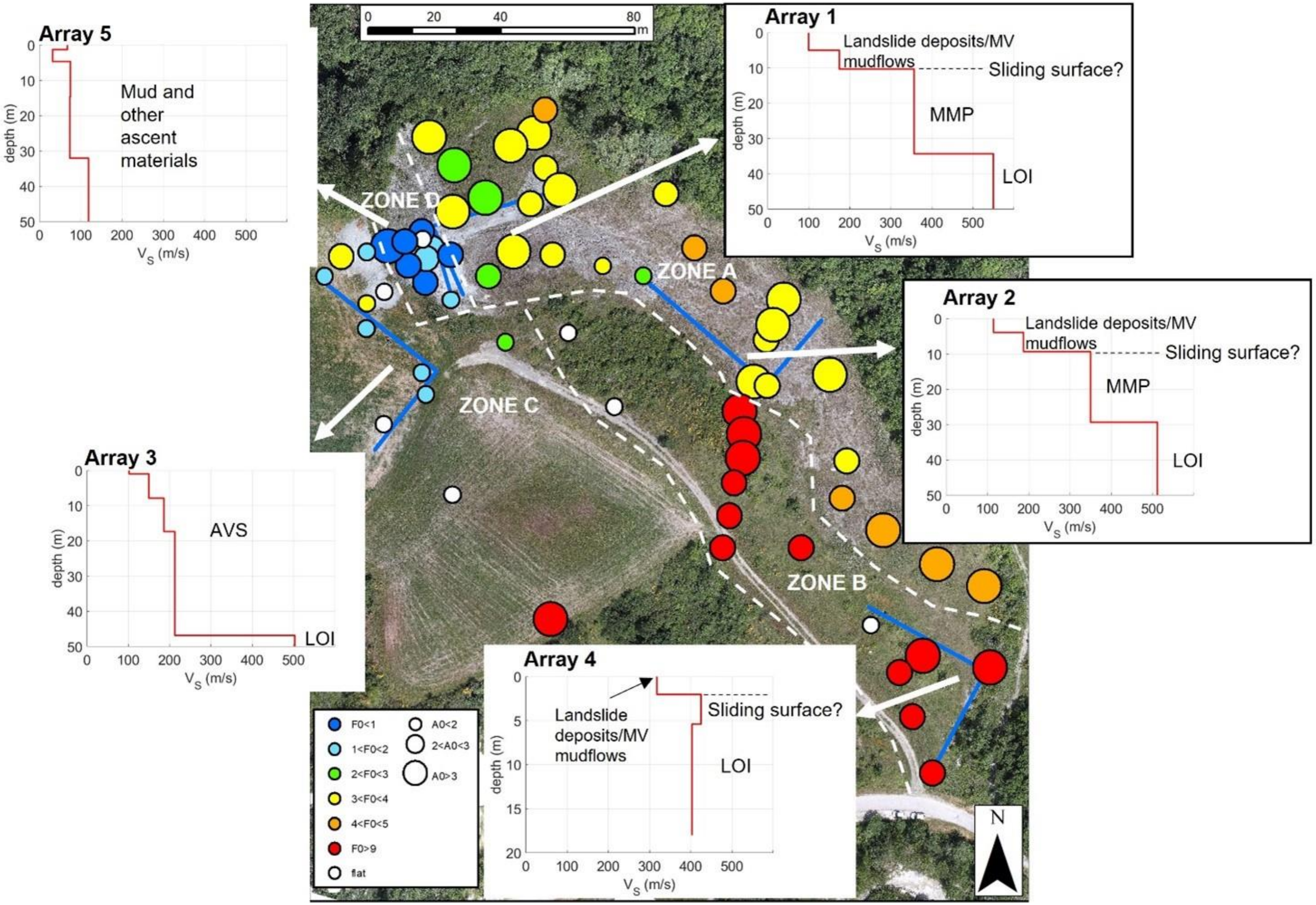

Zone A: Landslide deposits (F0: 3–4 Hz) with strong impedance contrasts at 10 m depth.

Zone B: Southern/western flanks with flat curves or F0 > 9 Hz, indicating no resonant interfaces.

Zone C: Argille Varicolori with low-amplitude peaks (F0: 2–4 Hz).

Zone D: Mud volcano area (F0 < 2 Hz) linked to shallow interfaces.

Stability Analysis: General Workflow

1.

Slope Geometry
Collect topography / bathymetry data

2.

Soil Parameters
Define geotechnical properties (friction angle ϕ, cohesion c, density γ, ...)

3.

Slip Surface Hypothesis
Assume potential failure geometry
(e.g., circular arc or prescribed shape based on geological information)

4.

External Loads
Apply seismic input, water loading, etc.

$$\textbf{SAFETY FACTOR (FoS)} = \frac{\text{forces resisting movement}}{\text{forces driving movement}}$$

> 1 STABLE SLOPE

< 1 UNSTABLE SLOPE

ALMA MATER STUDIORUM
UNIVERSITÀ DI BOLOGNA

Stability Analysis

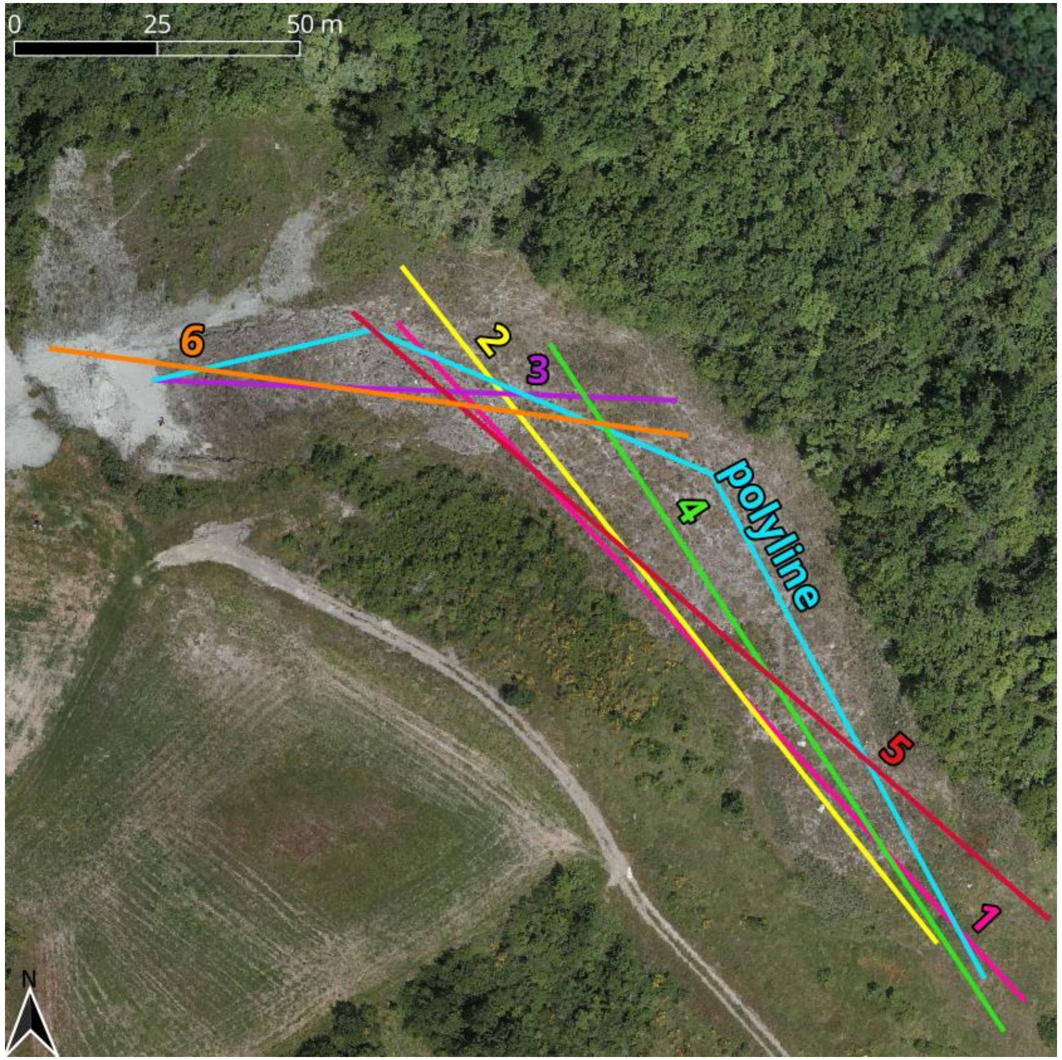

- 7 profiles
- Sensitivity analysis on geotechnical parameters

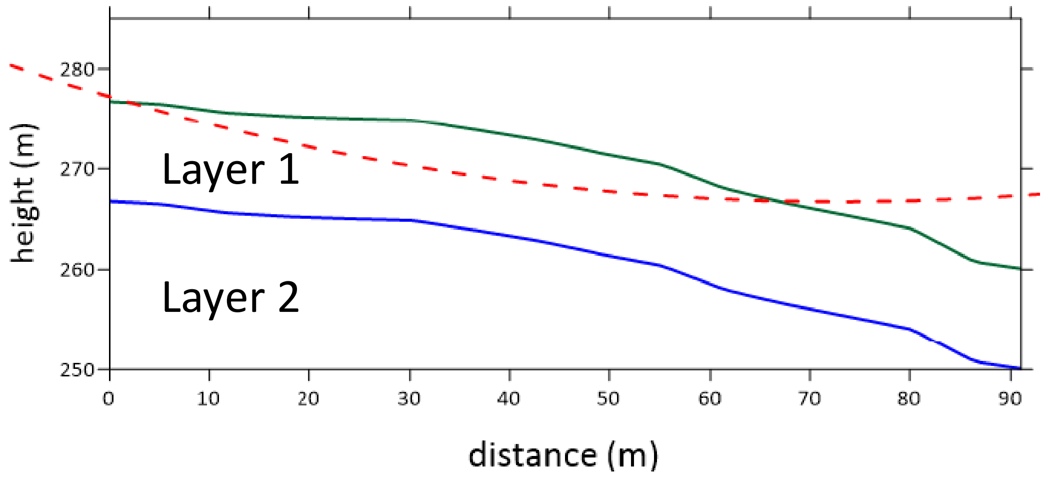

	Case 1	Case 2	Case 3	Case 4	Case 5
Layer 1	γ_1= 18.5 kN/m³ ϕ_1= 21° c_1= 18 kPa	γ_1= 16 kN/m³ ϕ_1= 18° c_1= 10 kPa	γ_1= 13 kN/m³ ϕ_1= 16° c_1= 4 kPa	γ_1= 10 kN/m³ ϕ_1= 10° c_1= 3 kPa	γ_1= 15 kN/m³ ϕ_1= 5° c_1= 5 kPa
Layer 2	γ_2= 20 kN/m³ ϕ_2= 21° c_2= 21.5 kPa	γ_2= 20 kN/m³ ϕ_2= 21° c_2= 21.5 kPa	γ_2= 20 kN/m³ ϕ_2= 21° c_2= 21.5 kPa	γ_2= 20 kN/m³ ϕ_2= 21° c_2= 21.5 kPa	γ_2= 20 kN/m³ ϕ_2= 21° c_2= 21.5 kPa

Stability Analysis

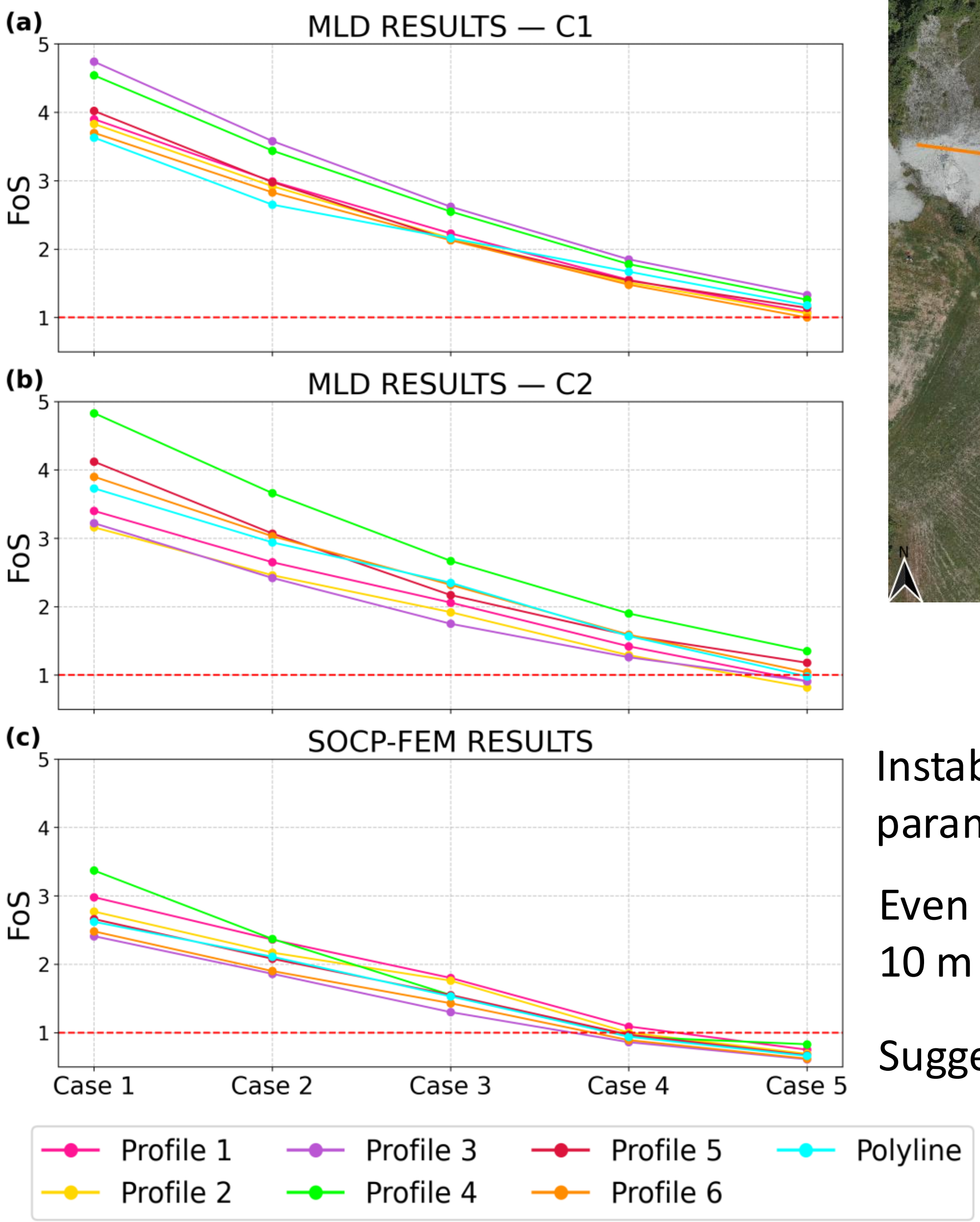

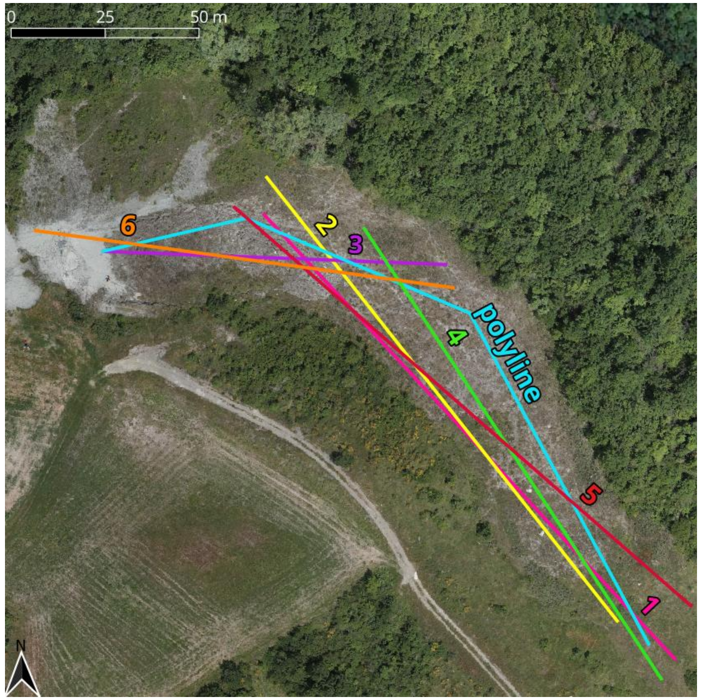

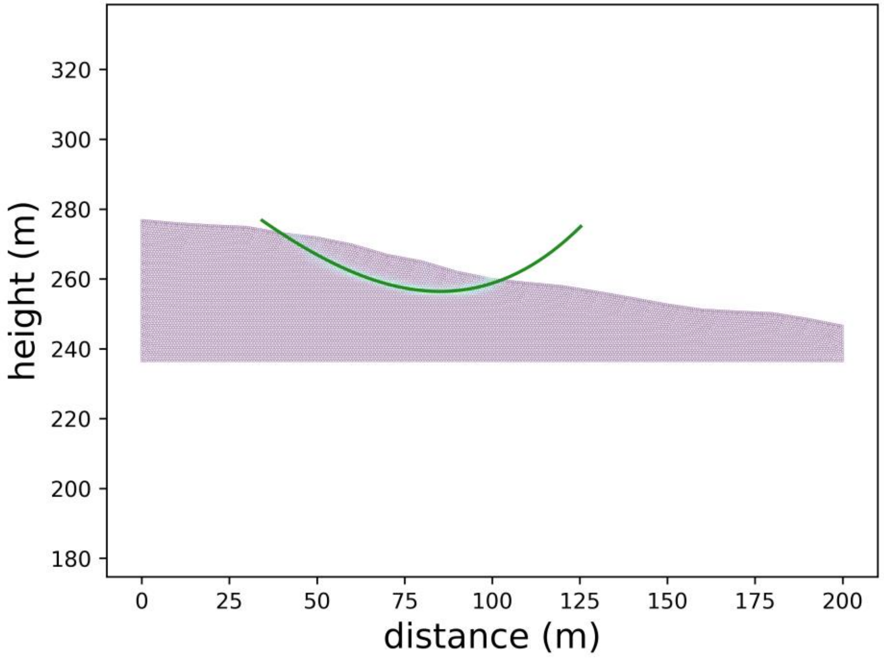

Polyline - Case 5 (max thickness~ 8 m)

Instability occurs only in specific conditions: deeper slip surfaces + unfavorable parameters

Even when instability occurs, the extracted sliding surfaces do not align with the 10 m interface

Suggests failure is more localized, not associated with a large-scale slip surface

ALMA MATER STUDIORUM
UNIVERSITÀ DI BOLOGNA

CONCLUSIONS

The regional geological map likely misclassifies the area as a landslide:
stability analysis suggests no evidence of large-scale failure at the 10 m interface.

The site appears stable under realistic conditions:
instability only occurs under extreme and unfavorable geotechnical assumptions.

Combining geophysical data with numerical modeling is key:
integrating seismic imaging and photogrammetry with slope stability simulations allows for more reliable interpretation.

Cross-validating field data with numerical modelling should become standard practice
for reliable geohazard assessment and effective decision-making.

ALMA MATER STUDIORUM
UNIVERSITÀ DI BOLOGNA

Tsunamis

- Tsunamis are polychromatic wavetrains generated by the movement of the entire water column
- Wavelengths of $10^2 \div 10^5$ m and periods of $10^2 \div 10^4$ s
- Around 75% are generated by earthquakes, but they also be caused by landslides, volcanic eruptions, atmospheric pressure, calving, asteroids, … (Levin et al. 2016)
- In the period 1997-2017, they caused US$280 billions in damages and more than 250 000 casualties (Imamura et al. 2019)

ALMA MATER STUDIORUM
UNIVERSITÀ DI BOLOGNA

The Great Wave off Kanagawa, Hokusai 1830-1831

- Very commonly used to represent tsunamis
- Definitely **NOT** a tsunami!
- It is a *rogue wave*, i.e. a wind wave with anomalously large amplitude

What a tsunami really looks like: Shoaling and Amplification

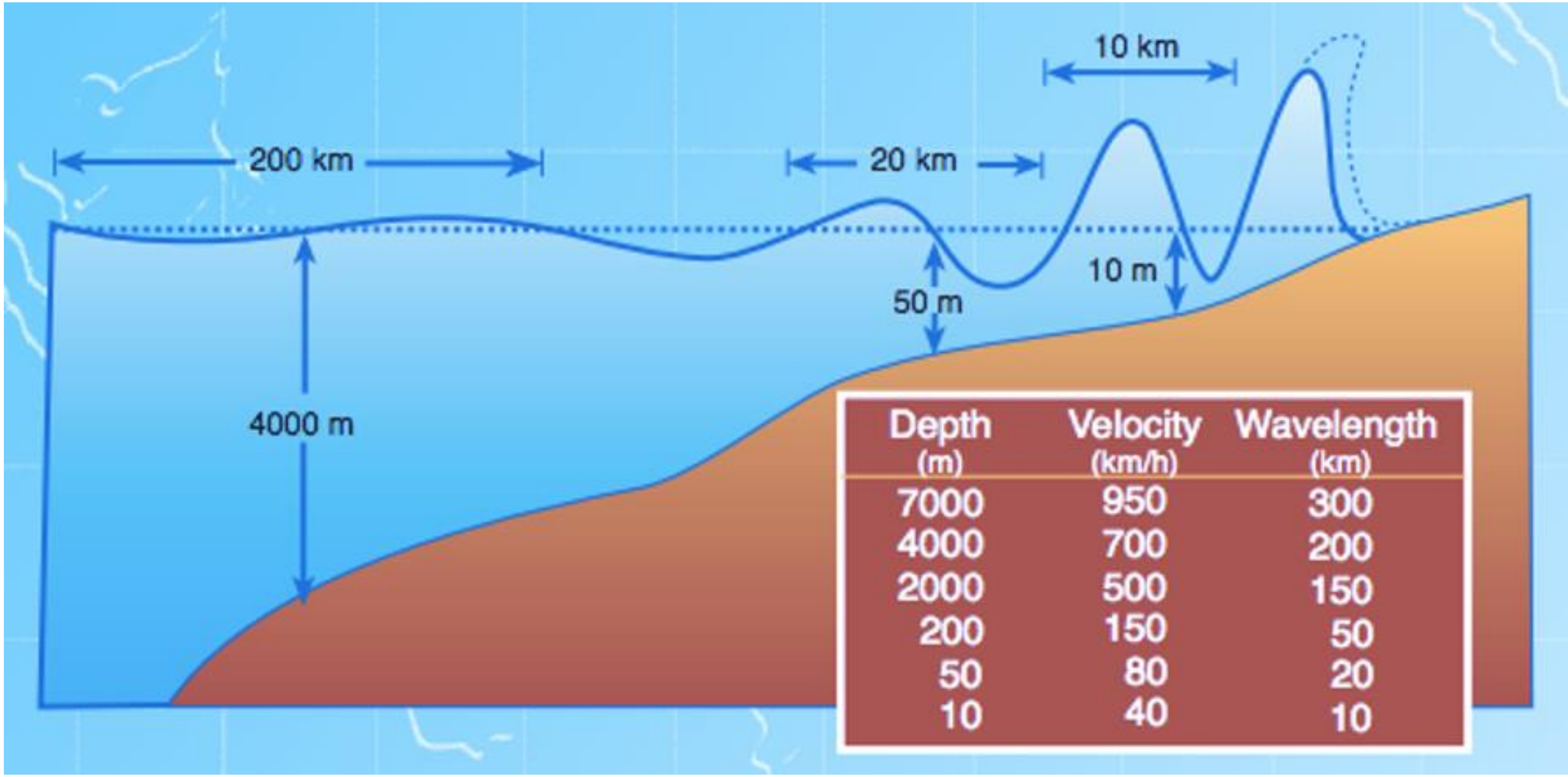

Intergovernmental Oceanographic Commission. 2012. Tsunami, The Great Waves, Second Revised Edition. Paris, UNESCO, 16 pp., illus. IOC Brochure 2012-4. (English.)
http://itic.ioc-unesco.org/index.php?option=com_content&view=article&id=1169&Itemid=1137&lang=en

Costliest Tsunamis

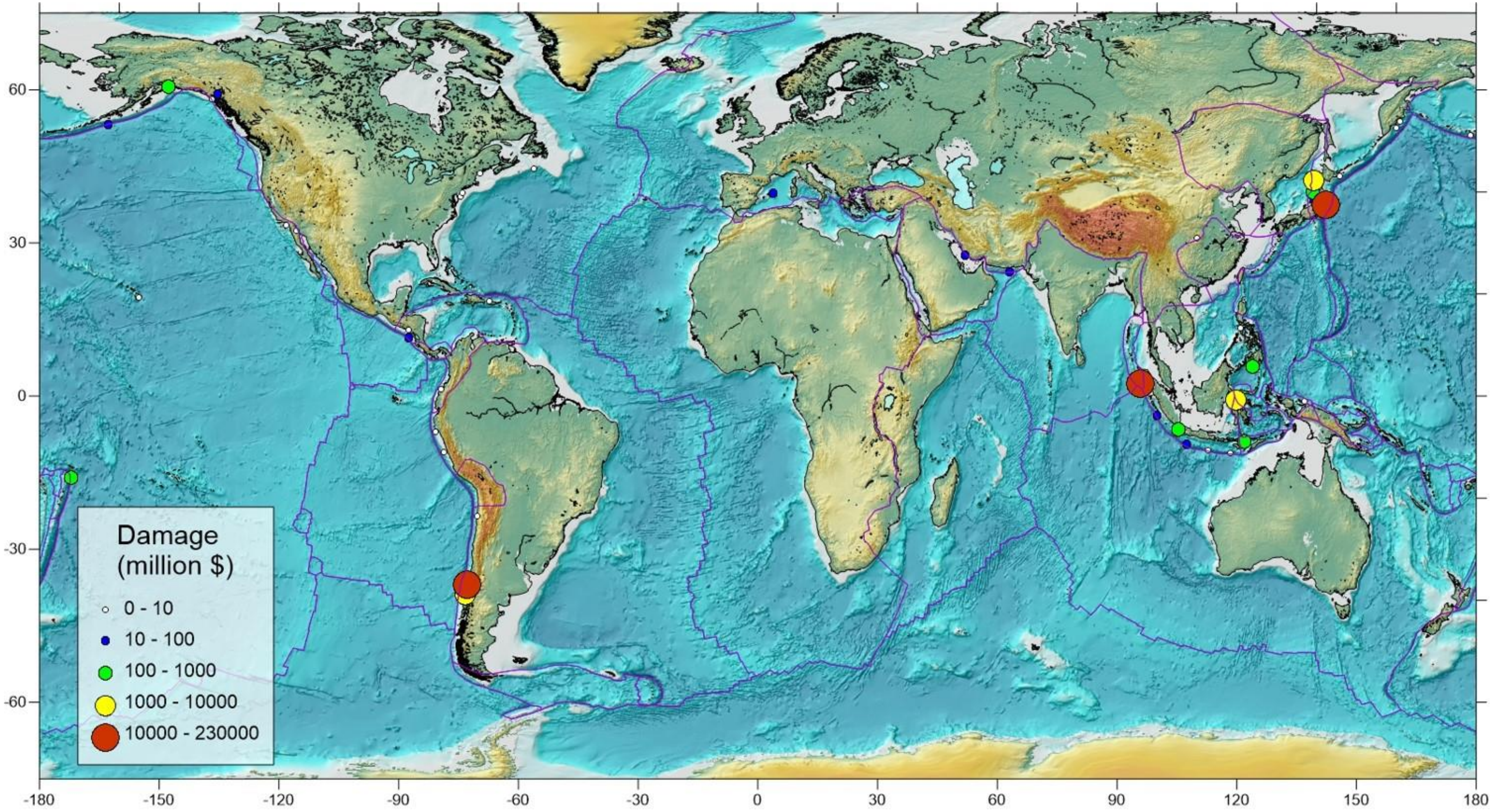

- Tohoku tsunami, Honshu island, Japan 11/03/2011 US$220B
- Maule tsunami, Central Chile 27/02/2010 US$30B
- Sumatra tsunami, Indonesia 26/12/2004 US$10B

Deadliest tsunamis

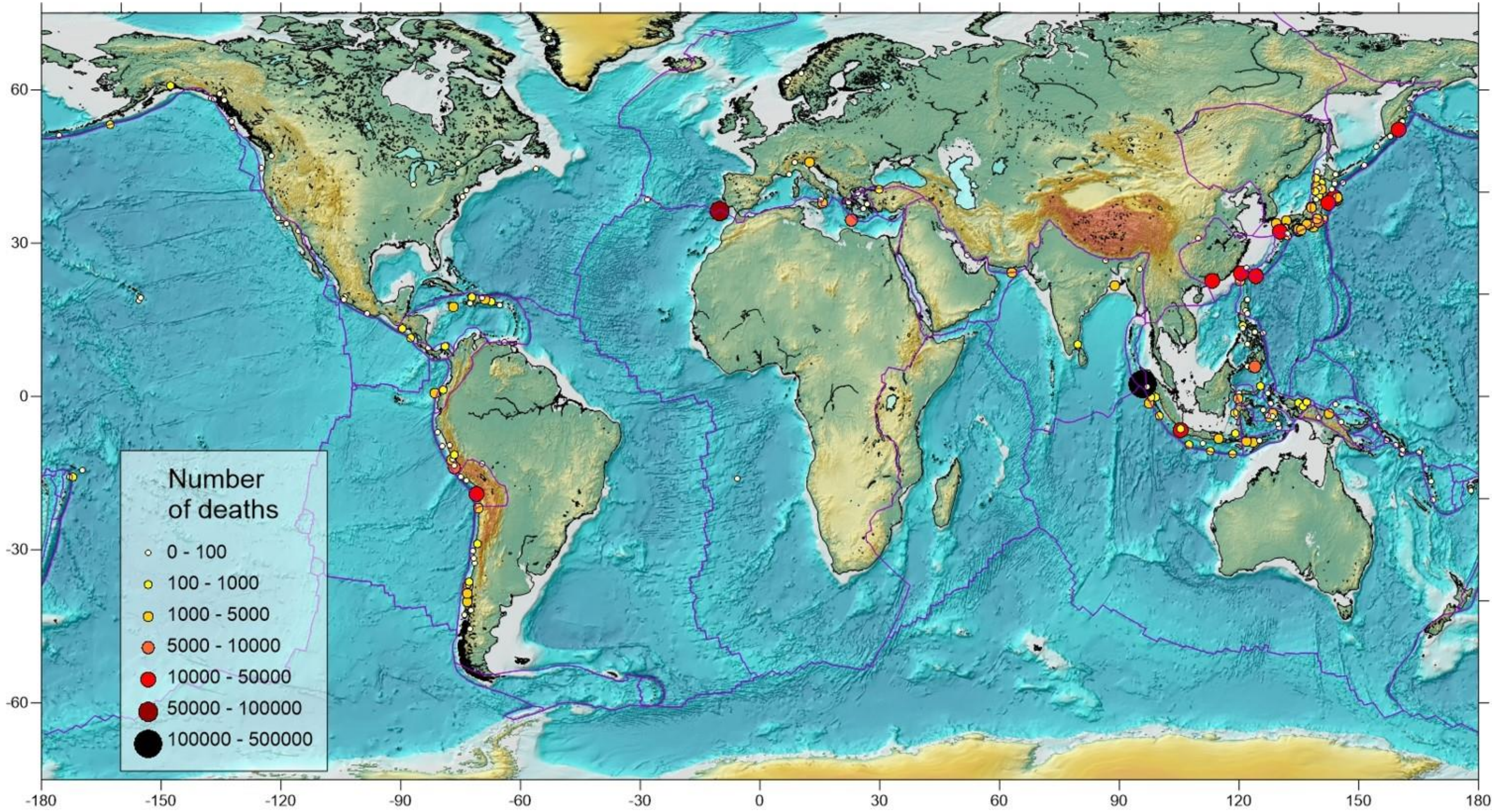

- Sumatra tsunami, Indonesia 26/12/2004 230 000 casualties
- Lisbon, Portugal 1/11/1755 50 000 casualties
- Taiwan strait tsunami 22/5/1782 40 000 casualties

The 2011 Tohoku tsunami is in seventh place.

What a tsunami really looks like: Inundation

From “3/11 — The Tsunami: The First 3 Days”, available at https://www.youtube.com/watch?v=0E2Q7kr4L2c?t=18m10s

Tsunami Travel Times

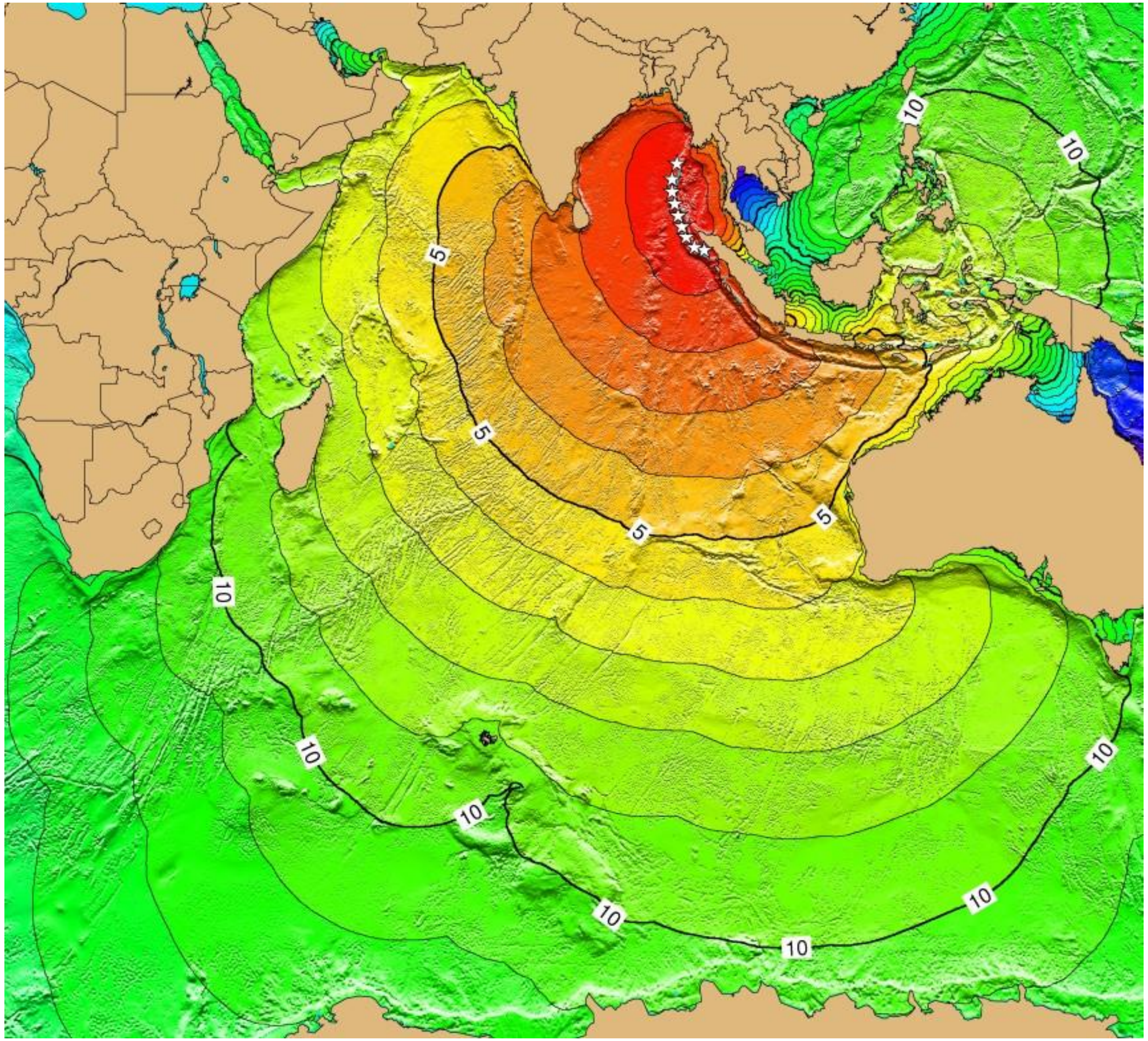

Travel time map for the 2004 Sumatra tsunami, from https://www.ncei.noaa.gov/products/natural-hazards/tsunamis-earthquakes-volcanoes/tsunamis/travel-time-maps

- Most casualties occurred in Indonesia
- Thousands of casualties also in India and Sri Lanka, which are **hours** away from the source
- Few casualties also in the coasts of east Africa

Tsunamis Early Warning Systems

- Need to work in a window of minutes (near-field) or hours (far-field) in order to issue timely warnings
- Mostly based on seismic data (Amato et al. 2021; Duputel et al. 2011; Lomax & Michelini 2013)
- Benefit greatly from direct tsunami measurements (Rabinovich & Eblé 2015)
- Recent developments in data assimilation methods (Maeda et al. 2015) and Bayesian forecasting (Selva et al. 2021) benefit greatly from direct tsunami measurements

ALMA MATER STUDIORUM
UNIVERSITÀ DI BOLOGNA

Tide Gauges

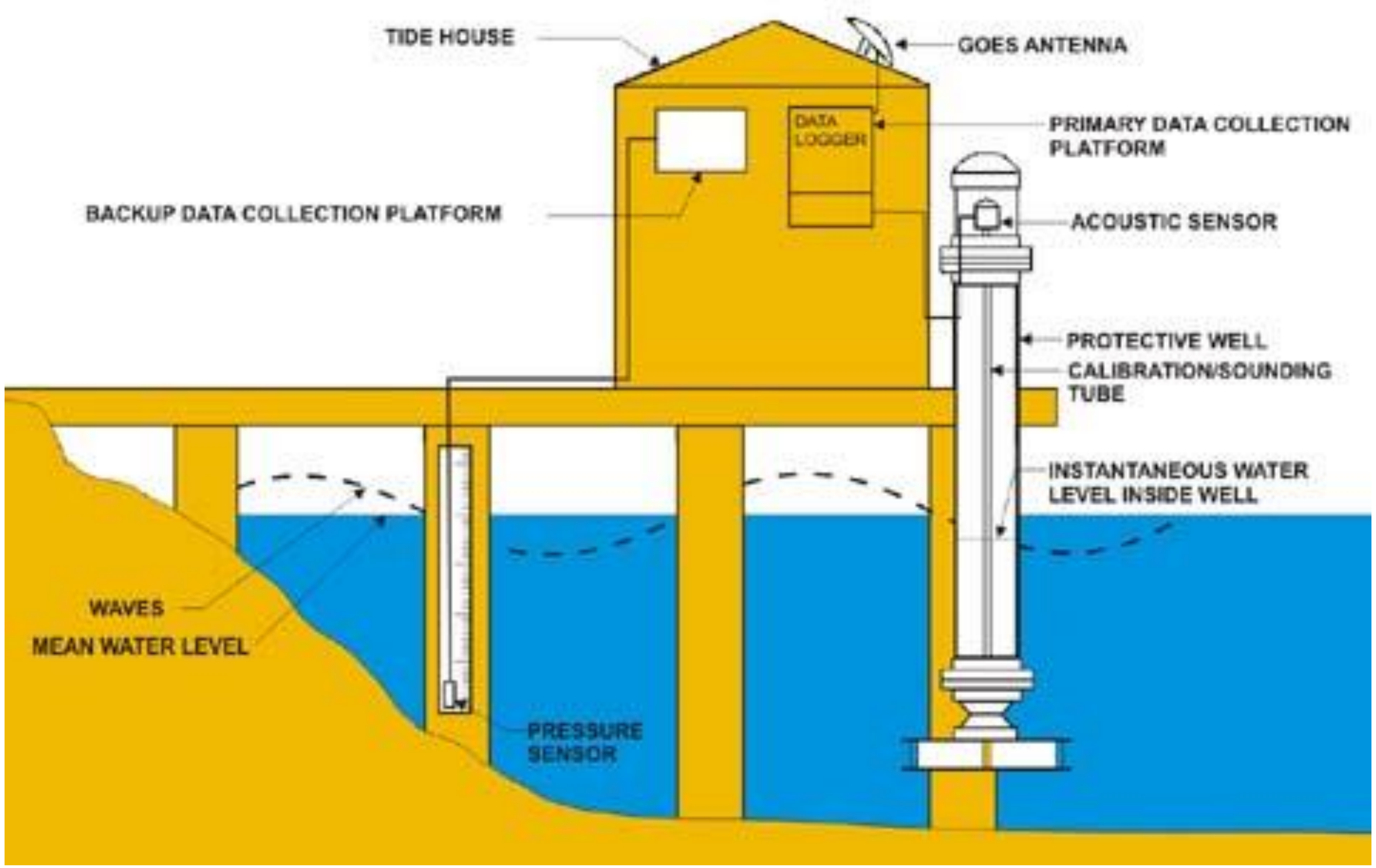

- Tide Gauges have been used since the 1800s to measure tides
- Old ones used floats, more modern ones use acoustic measurements
- Tide gauge records are available for very old events (Krakatoa 1883, Ligurian Sea Earthquake 1887)
- Too close to shore for early warning, but used to confirm issued warnings

From https://oceanservice.noaa.gov/education/tutorial_tides/tides11_newmeasure.html

Tide Gauges

Stazione meteomarina installata a Thule, progetto MACMAP

Today, many stations use radar sensors to measure the sea level, which allow for larger sampling rates

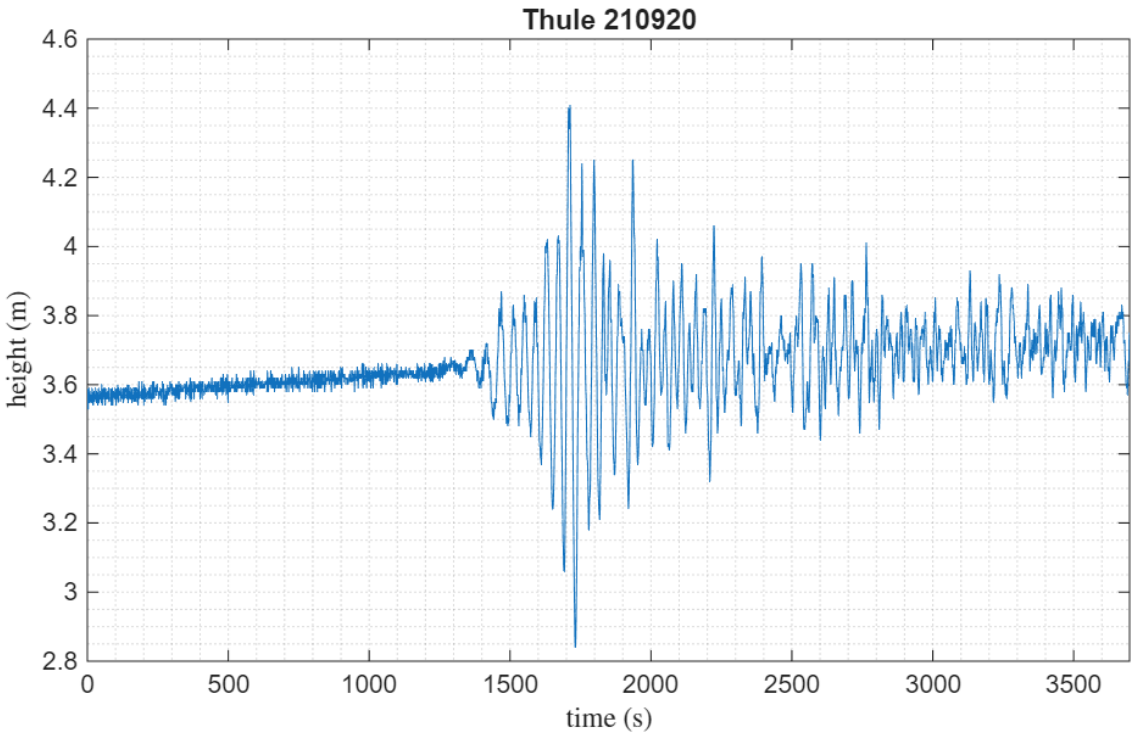

ALMA MATER STUDIORUM
UNIVERSITÀ DI BOLOGNA

Tide Gauges for TEW in the Mediterranean

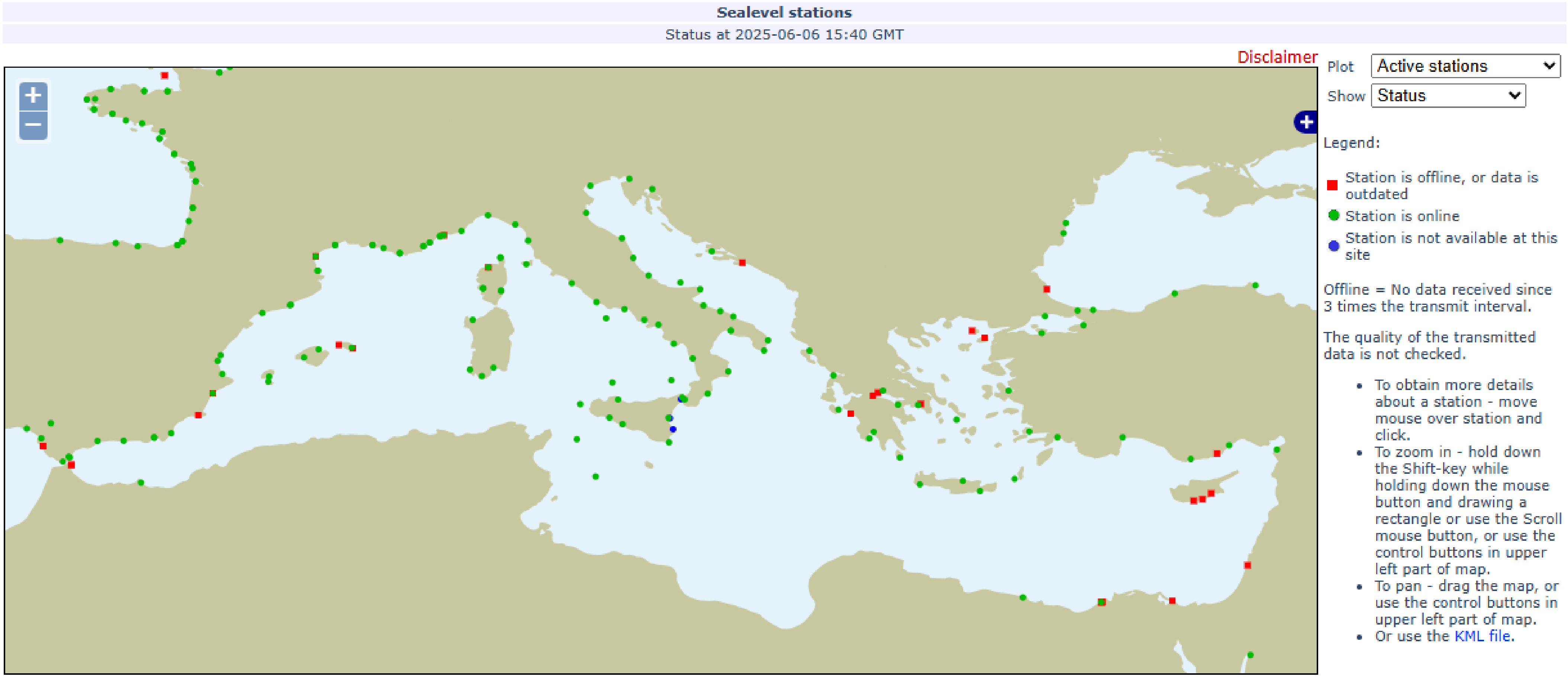

Web portal for IOC Sea Level Monitoring Facilty data, available at https://www.ioc-sealevelmonitoring.org/map.php.

Among others, it includes data from the DART network and from ISPRA tide gauge network.

Ocean Bottom Pressure Gauges

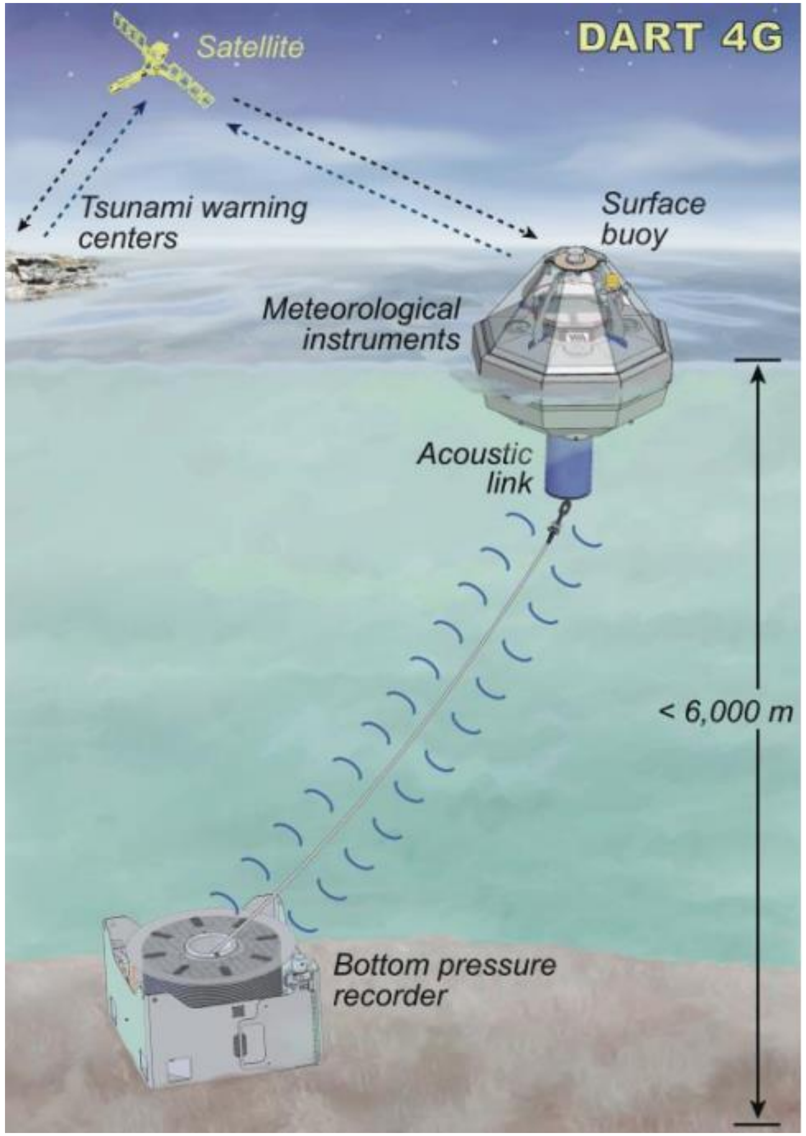

Structure of a DART 4G OBPG, developed by PSMSL.

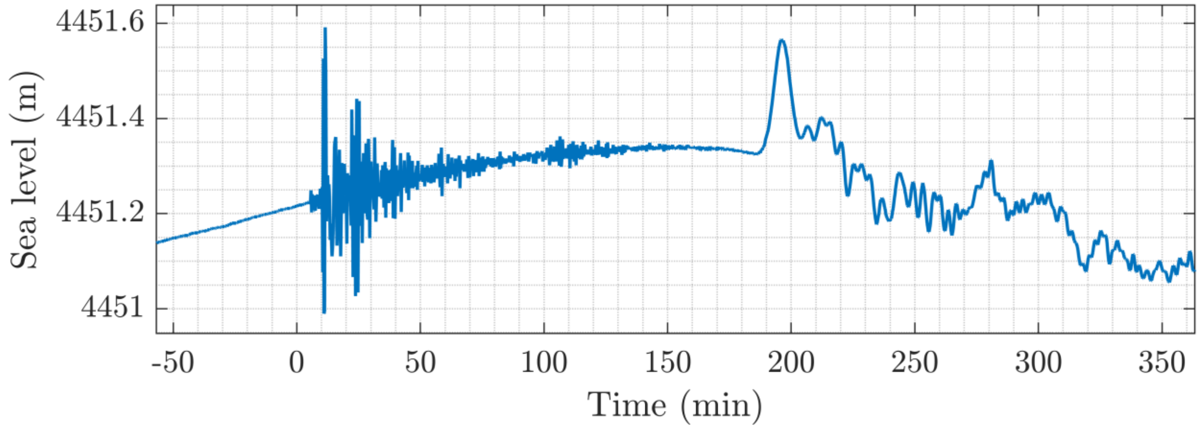

27/10/2010 06:34:15 UTC MW = 8.8 Chilean earthquake, DART 32412.

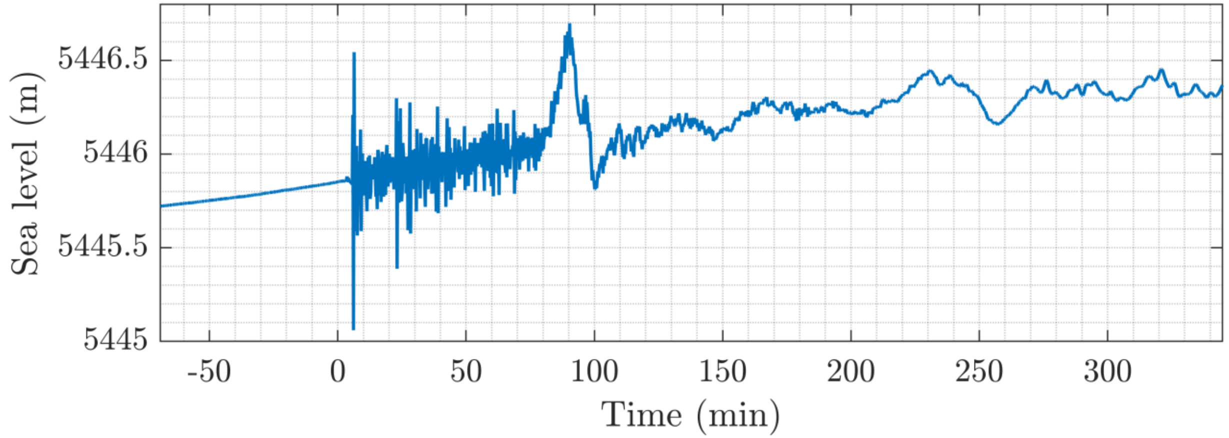

11/03/2011 05:46:23 UTC MW = 9.1 Tohoku earthquake, DART 21419.

ALMA MATER STUDIORUM
UNIVERSITÀ DI BOLOGNA

OBPG Networks

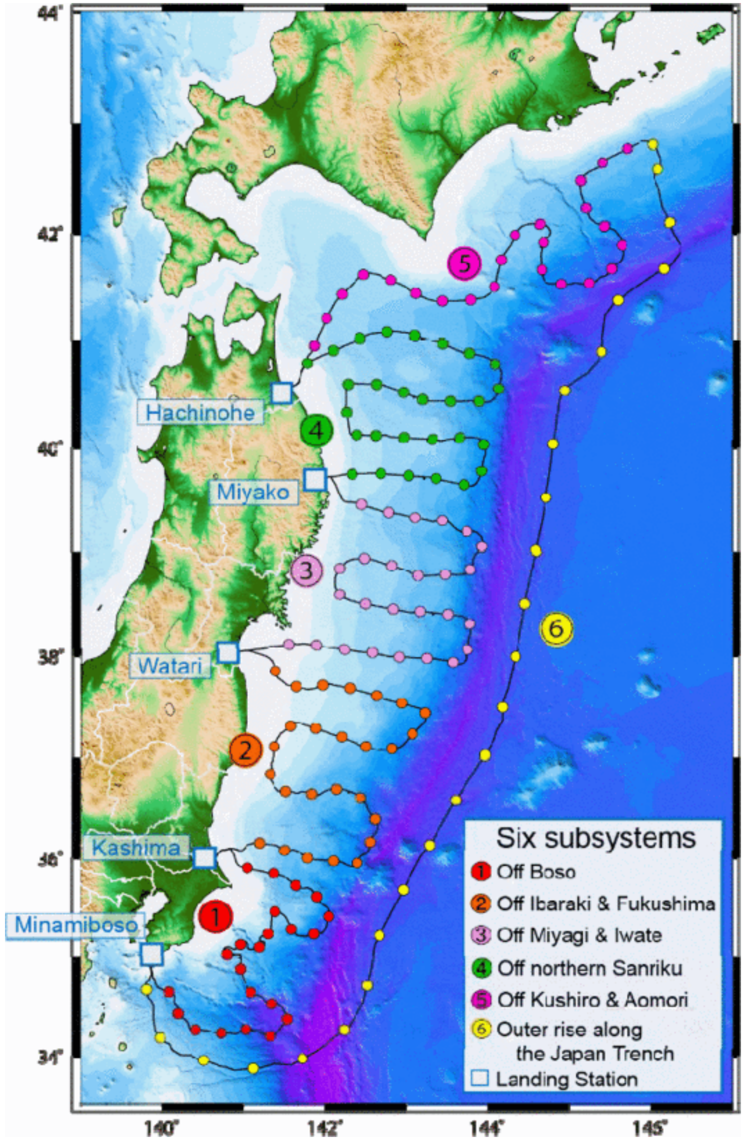

Map of the cabled OBPGs and seismometers of the S-Net (Mochizuki et al. 2018)

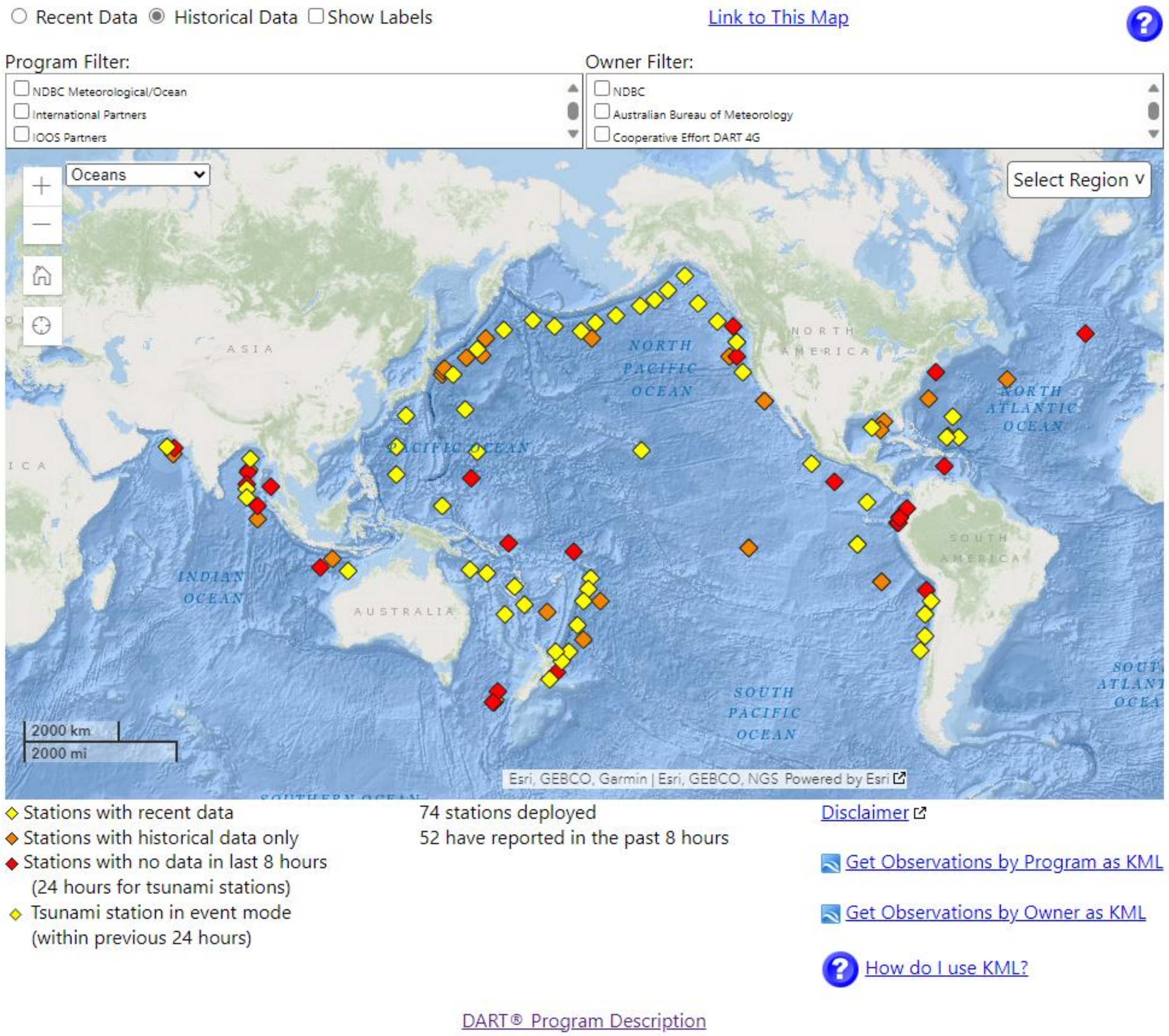

Web interface for NOAA's DART network data (Titov et al. 2005), available at https://www.ndbc.noaa.gov/obs.shtml?lat=13&lon=-173&zoom=2&pgm=tsunami

GNSS buoys

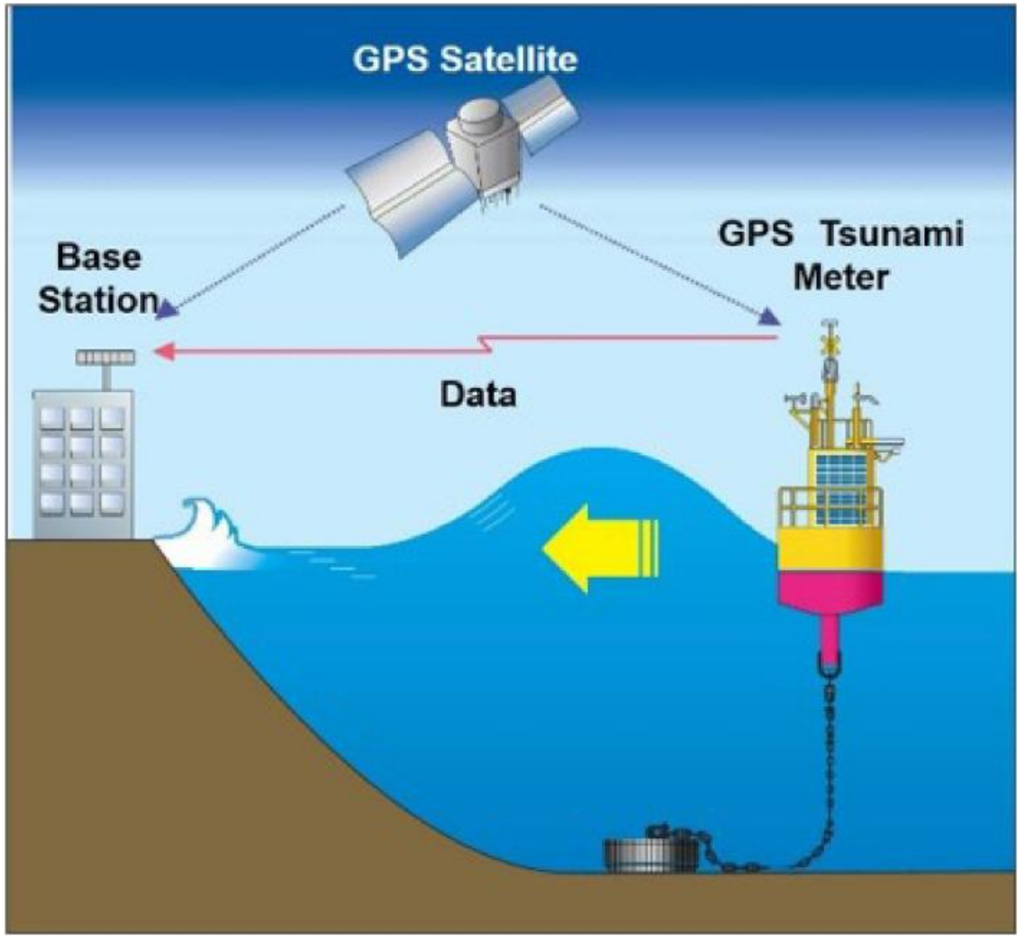

Principles behind GNSS buoys for sea level measurement

GNSS buoys offshore of Ofunato

Images from Kato et al. 2022

Tsunami Detection from Satellites

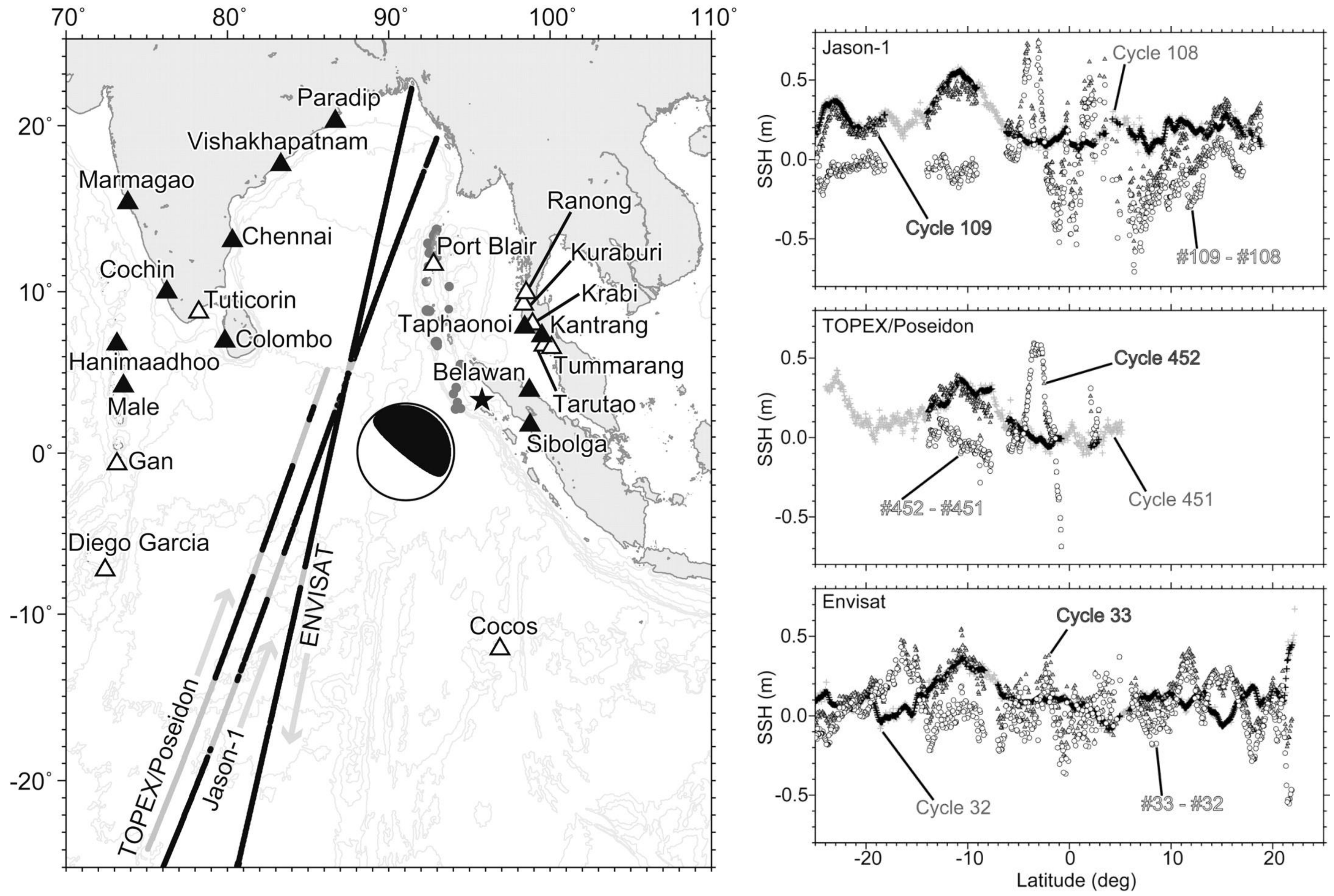

- There have been instances of large tsunamis observed by satellite altimetry data
- They provide «snapshots» of propagation
- Density in observations and the time needed to process data makes it not suitable for TEWS

Images from Fujii & Satake 2007

Other methods

- Observations of tsunami signatures in the ionosphere, retrieved through GNSS data (Ravanelli et al. 2021)
- Inversion of electromagnetic signals induced by the tsunami propagation, measured from seafloor EM stations (Baba et al. 2024)
- Observations of horizontal ground displacement caused by the tsunami load through seismometers (Okal 2007)

ALMA MATER STUDIORUM
UNIVERSITÀ DI BOLOGNA

Conclusions

- Sea level monitoring is the most important component for both retrospective and real-time tsunami analysis
- The integration of many types of instruments allows for great coverage for early warning purposes
- Though some areas are still lacking fundamental instrumentation, great progress is continuously being made, e.g. new OBPGs in the Ionian Sea are about to be deployed
- Non traditional tsunami measurement methodologies might further improve real-time operation in the near future

References

[1] A. Mazzini and G. Etiope, “Mud volcanism: An updated review”, Earth-Science Reviews, vol. 168, pp. 81–112, 2017.
[2] L. I. Dimitrov, “Mud volcanoes—the most important pathway for degassing deeply buried sediments”, Earth-Science Reviews, vol. 59, no. 1-4, pp. 49–76, 2002.
[3] G. Martinelli, S. Cremonini, E. Samonati et al., Geological and geochemical setting of natural hydrocarbon emissions in Italy. InTech Rijeka, Croatia, 2012.
[4] Dal Moro, G., Moura, R. M. M., & Moustafa, S. S. (2015). Multi-component joint analysis of surface waves. Journal of Applied Geophysics, 119, 128-138.
[5] S. Tinti and A. Manucci, “Gravitational stability computed through the limit equilibrium method revisited”, Geophysical Journal International, vol. 164, no. 1, pp. 1–14, 2006.
[6] S. Tinti and A. Manucci, “A new computational method based on the minimum lithostatic deviation (MLD) principle to analyse slope stability in the frame of the 2-D limit-equilibrium theory”, Natural Hazards and Earth System Sciences, vol. 8, no. 4, pp. 671–683, 2008.
[7] L. Wang, X. Zhang, and S. Tinti, “Shallow landslides modeling using a particle finite element model with emphasis on landslide evolution”, Earth Surface Dynamics Discussions, vol. 2019, pp. 1–19, 2019.
[8] Levin, B. W., Nosov, M., Levin, B. W., & Nosov, M. A. (2016). Hydrodynamic Processes at the Source of a Tsunami of Seismotectonic Origin: Incompressible Ocean. Physics of Tsunamis, 89-180.
[9] Imamura, Fumihiko et al. (2019). “Recent occurrences of serious tsunami damage and the future challenges of tsunami disaster risk reduction”. In: Progress in Disaster Science 1, p. 100009.
[10] Amato, Alessandro et al. (2021). “From seismic monitoring to tsunami warningin the Mediterranean Sea”. In: Seismological Research Letters 92.3, pp. 1796–1816.
[11] Duputel, Zacharie et al. (2011). “Real-time W phase inversion during the 2011 off the Pacific coast of Tohoku Earthquake”. In: Earth, planets and space 63.7,pp. 535–539.
[12] Lomax, Anthony and Alberto Michelini (2013). “Tsunami early warning within five minutes”. In: Pure and Applied Geophysics 170, pp. 1385–1395.
[13] Rabinovich, Alexander B and Marie C Ebl´e (2015). “Deep-ocean measurements of tsunami waves”. In: Pure and Applied Geophysics 172, pp. 3281–3312.
[14] Maeda, Takuto et al. (2015). “Successive estimation of a tsunami wavefield without earthquake source data: A data assimilation approach toward real-time tsunami forecasting”. In: Geophysical Research Letters 42.19, pp. 7923–7932.
[15] Selva, Jacopo et al. (2021). “Probabilistic tsunami forecasting for early warning”. In: Nature communications 12.1, p. 5677. doi: 10.1038/s41467-021-25815-w.
[16] Titov, V., Rabinovich, A. B., Mofjeld, H. O., Thomson, R. E., & González, F. I. (2005). The global reach of the 26 December 2004 Sumatra tsunami. Science, 309(5743), 2045-2048.
[17] Kato, T., Terada, Y., Tadokoro, K., & Futamura, A. (2022). Developments of GNSS buoy for a synthetic geohazard monitoring system. Proceedings of the Japan Academy, Series B, 98(2), 49-71.
[18] Fujii, Y., & Satake, K. (2007). Tsunami source of the 2004 Sumatra–Andaman earthquake inferred from tide gauge and satellite data. Bulletin of the Seismological Society of America, 97(1A), S192-S207.
[19] Ravanelli, M., Occhipinti, G., Savastano, G., Komjathy, A., Shume, E. B., & Crespi, M. (2021). GNSS total variometric approach: first demonstration of a tool for real-time tsunami genesis estimation. Scientific reports, 11(1), 3114.
[20] Baba, T., Lin, Z., Minami, T., & Toh, H. (2024). Harnessing electromagnetic data for tsunami source estimation: a comprehensive review. Philosophical Transactions A, 382(2286), 20240082.
[21] Okal, E. A. (2007). Seismic records of the 2004 Sumatra and other tsunamis: A quantitative study. In Tsunami and Its Hazards in the Indian and Pacific Oceans (pp. 325-353). Birkhäuser Basel.